IEEE Access
Multidisciplinary | Rapid Review | Open Access Journal

Received February 3, 2020, accepted March 1, 2020, date of publication March 9, 2020, date of current version March 23, 2020.

Digital Object Identifier 10.1109/ACCESS.2020.2979683

Statistical Analysis of Rain at Millimeter Waves in Tropical Area

AHMED M. AL-SAMAN[1], MICHAEL CHEFFENA[1], MARSHED MOHAMED[1], MARWAN HADRI AZMI[2], AND YUN AI[1]

[1]Department of Manufacturing and Civil Engineering, Norwegian University of Science and Technology (NTNU), 2815 Gjøvik, Norway
[2]Wireless Communication Centre, School of Electrical Engineering, Faculty of Engineering, Universiti Teknologi Malaysia, Johor Bahru 81310, Malaysia

Corresponding author: Ahmed M. Al-Saman (ahmed.al-saman@ntnu.no)

This work was supported in part by H2020-MSCA-RISE-2015 under Grant 690750, in part by Universiti Teknologi Malaysia (UTM) under Grant Q.J091300.23C9.00D96, in part by CRG under Grant R.J130000.7351.4B468, in part by HICOE under Grant R.J130000.7851.4J413, in part by MOHE through FRGS-UTM under Grant R.J130000.7851.5F177, and in part by the Manu Lab, NTNU, Gjøvik.

ABSTRACT The high frequencies of millimeter wave (mm-wave) bands have been recognized for the fifth generation (5G) and beyond wireless communication networks. However, the radio propagation channel at high frequencies can be largely influenced by rain attenuation, especially in tropical regions with high rainfall intensity. In this paper, we present the results of rainfall intensity and rain attenuation in tropical regions based on one-year measurement campaign. The measurements were conducted from September 2018 until September 2019 at 21.8 GHz (K-band) and 73.5 GHz (E-band) in Malaysia. The rainfall intensity was collected using three rain gauges installed along a 1.8 km link. The rain attenuation is computed from the difference between the measured minimum received signal level (RSL) during clear sky and rain conditions. The measured rain rate and rain attenuation distributions are then analysed and benchmarked with several previous measurements and well-known prediction models such as the ITU-R P. 530-17. The rainfall rate results showed that the best agreement between the measured rainfall rate in Malaysia and the ITU-R PN.837-1 prediction value for Zone P is up to 0.01% of time (99.99% of time agrees well and only disagrees for 0.01% of time). For the E-band, the maximum measured rain attenuation exceeding 0.03% of the year is around 40.1 and 20 dB for 1.8 and 0.3 km links, respectively, at the maximum rain rate of 108 mm/h. For the K-band, the maximum rain attenuation exceeding 0.01% of the year is around 31 dB for the 1.8 km link. Finally, the rain rates exceeding 108 and 180 mm/h at 73.5 and 21.8 GHz, respectively, along the 1.8 km path caused an outage on our measurement setup. The rain rate of 193 mm/h and above caused an outage for the 0.3 km E-band link. The experimental data as well as the presented data analysis can be utilized for efficient planning and deployments of mm-wave wireless communication systems in tropical regions.

INDEX TERMS Mm-wave, rain attenuation, propagation, E-band, K-band, 73.5 GHz, tropical area.

I. INTRODUCTION

Radio communication frequencies are being expanded to millimeter waves (mm-wave) in order to occupy a larger bandwidth. Using mm-wave frequencies in 5G wireless networks will solve the spectrum shortage of existing 4G cellular communication systems operating at frequencies below 6 GHz [1]. Mm-wave bands will be used for different outdoor scenarios such as backhaul and fixed wireless communication to provide high data rates for various applications [2]. In reality, 5G standardization has already started, with a focus on gigabit coverage between 28 GHz and 39 GHz bands [3]. However, there is still a profusion of spectrum beyond these bands, specifically at 70 GHz (71–76 GHz) and 80 GHz (81–86 GHz). The mm-wave bands up to 52.6 GHz have been envisioned by 3GPP Release 15. With Release 17, 3GPP would like to extend that across 52.6 GHz all the way up to 114 GHz [4]. However, the quality of the radio link at high frequencies can be potentially affected by weather conditions such as rain, snow and fog, which should be considered in the link budget [5], [6]. Due to absorption and scattering at frequencies above 10 GHz, the precipitations cause

The associate editor coordinating the review of this manuscript and approving it for publication was Jules Merlin Moualeu.

significant attenuation at these frequencies, especially at the E-band [1].

Comprehension of atmospheric propagation effects in mm-wave bands is required, especially in the case of rain. Rain is one of the primary factors that cause of attenuation at these bands since the wavelength of propagation is comparable to the size of the rain droplet [7]. Numerous measurements have been conducted to study the effects of rain on both satellite and terrestrial communications.

In satellite communication, several studies on the effect of rain have been conducted in Europe on the microwave band from 10 to 40 GHz [8]–[10]. The complementary cumulative distribution functions (CCDFs) were computed for rainfall rate and rain attenuation over four years (2009-2013) of Earth-space propagation experiments at 19.7 and 20.2 GHz in the southwest of France [8]. Also in France, rain rate and attenuation were measured at 20.2 GHz based on Amazonas 3 satellite links over one year (2017) [9]. The rain attenuation was calculated based on two slant satellite links (19.698 and 39.402 GHz) propagation experiments in Madrid, Spain over three years (2014-2017) [10].

Unlike Europe, tropical countries often experience heavy rain occurrences, hence, studies conducted in Europe would be insufficient. Video streaming was performed over a high-speed link via the WINDS satellite in a tropical area (Singapore) to investigate the effects of rainfall on the signal strength of the link and the video quality [11]. The rain induced scintillation was studied based on attenuation measurement over a one year period during 2011 and 2012, from MEASAT3 satellite at Ku-band (12-18 GHz) in Malaysia [12]. In [13], the performance of the Silva Model in [14] for rain attenuation prediction in slant paths for satellite links was investigated and compared to the ITU-R P.618-11 model [15] based on data from three slant paths in tropical regions of Malaysia [16], [17] and Australia [18].

This paper investigates rain attenuation on terrestrial links. An overview of most previous works on rain attenuation in terrestrial links is presented in the following Section.

II. RELATED WORK

Many years ago, rain attenuation on terrestrial links was studied at microwave bands below 30 GHz and mm-wave bands. In [19], the rain attenuation prediction model was proposed and developed using geophysical observations of the statistics of point rain rate, the horizontal structure of rainfall, and the vertical temperature structure of the atmosphere. The space-time correlation of rain attenuation was investigated in [20] based on 42 GHz starlike network measurements in Norway. In [21], different rain attenuation prediction methods were reviewed and compared. The improvement of rain attenuation prediction methods was proposed by [22] and compared with experimental data collected from 30 terrestrial radio links for path lengths ranging from 1.3 to 58 km, and for frequency bands from 7 to 38 GHz, located in Africa, Europe, North America, and Japan.

In the last century, studies of rain attenuation on terrestrial links have been conducted at mm-wave frequencies of various distances and locations. At 0.4 km path length, the rain attenuation was measured in [23] at 48 GHz in New Jersey, United States (US). Researchers in [24] conducted similar measurements at 103 GHz in Japan, and at 120 GHz in [25] and [26]. The dependence of transmission distance on availability utilizing the statistical rain attenuation data was also investigated in these studies. Researchers in [27] and [28] conducted their studies on multiple frequencies in order to compare the effect of rain on different transmission frequencies at 0.8 km path length. The study in [27] was accomplished at 50.4, 81.8 and 140.7 GHz in Japan, while [28] achieved at 30, 50, 60, and 94 GHz in Belfort, France. For longer path distances, studies on rain attenuation were done at 1.97 km at 90.5 GHz in the USA [29], and at 6.5 km at 97 GHz in Portsmouth, UK [30]. Both studies used data collected for more than one year, in which statistical analysis and modeling of rain fade duration were presented. The following subsections provide an overview for most previous studies (to the authors knowledge) on rain attenuation at different bands.

A. KU, K AND KA-BANDS

The rainfall effects on wireless communication links have been studied at different regions of the world. The rainfall rate and rain attenuation measurements were accomplished at various tropical areas in six terrestrial line-of-sight (LOS) microwave links at 15 and 18 GHz in Brazil [31]–[33]. In [33], the obtained results based on a two-year measurement of these links indicated that the predicted rain attenuation using Crane [19] and ITU-R P.530-9 [34] models is underestimated for the tropical area. The review of rain attenuation studies from 1987 to 2005 based on long term measurements for frequencies between 10 and 38 GHz at 20 terrestrial links in Brazil were presented in [35]. In [36], Silva Mello *et al.* proposed prediction model to overcome the underestimation of the Crane and ITU-R prediction models for rain attenuation based on the rainfall rate distribution and concept of effective path length of rainfall rate. The proposed model was compared to the Crane [19] and ITU-R P.530-12 [37] models.

Rain attenuation effects were studied for several terrestrial links in tropical regions of Malaysia at different frequencies below 40 GHz. Various prediction models were reported in [38]–[54]. The frequency scaling of rain attenuation models was investigated based on a one year rain attenuation data measured at 23, 26, and 38 GHz in [38]. The path reduction factor models were analyzed in [39] and [42] based on rain attenuation data measured at 15 GHz in two different locations and over seven terrestrial links, respectively. Other studies conducted at 15 GHz were performed in [44], [45] on rain attenuation methods for terrestrial microwave links operating in tropical regions based on experimental rain rate and rain attenuation data over six terrestrial links. A study on rain attenuation statistics was conducted in [41] at 32.6 GHz with the link distance of 1.4 km.

In other tropical regions, studies were accomplished in Singapore [55], India [56], and Australia [57]. In [55], the rain attenuation was measured over ten years in the tropical region of Singapore at 15, 21, and 38 GHz for a 1.1 km link. The rain drop size distribution (DSD) was fitted with a negative-exponential distribution [55]. Rain attenuation was presented in [56] based on conducted measurement over one year at 11 GHz, on 3.2 km terrestrial link. The measured rain attenuation in [56] was compared with the empirical formula of specific attenuation in [58]. In [57], the rainfall rate and rain attenuation were presented based on conducted measurements over one year at 38 GHz along a 2.1 km terrestrial link. The results in [57] showed a significant difference between the ITU-R P.530-11 [59] fading prediction and the measured data.

For regions with four seasons, the rain attenuation was examined using different frequencies at K and Ka-bands in [60]–[69]. In [66] and [67], the rain attenuation was assessed for a 3.2 km experimental link at 18 GHz in South Korea, while the characteristics of seasonal rain attenuation were analyzed in South Africa based on measurements recorded for one year at 19.5 GHz along 6.73 km terrestrial link in [62] and [63]. The rain attenuation and its yearly variations was performed during a four-year period along 5.5 km link at 26 GHz in Prague, Czech Republic [65]. The statistics of the rain attenuation were presented based on two years of measurements at 30 GHz along 5.3 km terrestrial link in Italy [60]. In [61], the distribution of rain fade was proposed and compared to three years attenuation data at 38 GHz, 9 km terrestrial link, in the south east of United Kingdom (UK). The rainfall rate and rain attenuation were studied based on measurements at 23, 25, 28, and 38 GHz over 0.7 km terrestrial link in Beijing, China [68], [69].

B. E-BAND

The E-band (71-76 and 81-86 GHz) with a regulated bandwidth of 10 GHz is one of the future broadband communication bands [70]. The rain attenuation increases significantly with rising frequency, which restricts the path length of radio communication systems and limits the utilization of higher frequencies for LOS microwave links [69], [71], [72]. This makes the study of rain effects in the E-band crucial. A few studies have investigated the rain attenuation at the E-band, but mostly for short distances [5], [73]–[76]. In [5], the rainfall rate statistics and rain attenuation were investigated based on a one-year measurement data for a short 35 m link at 25.84 and 77.52 GHz in the UK. The rain attenuation at different rainfall rates for short measurement periods was studied at 77 and 300 GHz over 160 m terrestrial radars link in Birmingham, UK [73]. In [74], the attenuation measurements under extreme rain conditions in a climate wind tunnel were conducted to benchmark the possibility of wireless data transmission at 77 GHz during adverse weather conditions. The propagation loss with rain effect at 77 GHz was obtained over 180 m based on generated rain with rates of 33, 43, and 105 mm/h. The preliminary results of rain attenuation was presented in [75] based on short period of measurement at 73, 83, 148, and 156 GHz over a one year period in [76] at 73 and 83 GHz over a distance of 325 m in Milano, Italy.

Other studies that covered longer distances are found in [71], [72], [77], [78], which conducted at 0.84, 1, 3.2 and 3.45 km links, respectively. The impact of rain on signal attenuation for 75 GHz and 85 GHz bands was analyzed and modeled in [71] based on two years field measurements along 840 m link in Madrid, Spain. The impact of rain at 71-76 GHz bands was based on ten months of measurements of a 1 km terrestrial link in Molndal, Sweden [77]. Further measurements for mm-waves were accomplished in South Korea along 3.2 km experimental link at 75 GHz to study the impact of rain on signal propagation and to investigate the accuracy of the ITU-R models [72]. In [78] the rain attenuation was studied at 83.5 GHz based on one year measurement data conducted over a 3.45 km terrestrial link in Oslo, Norway.

Among the overviews of rain attenuation on terrestrial links at various frequencies of microwave and mm-wave bands in different regions worldwide, only few were conducted at E-band and none were in tropical regions. Malaysia is a tropical region with high rainfall rate of up to 280 mm/h. Previous studies in Malaysia on rain attenuation were based on measurements at 11, 15, 23, 26, 32 and 38 GHz and none had covered the E-band [38], [41], [46], [50].

To the best of our knowledge, this work is the only measurement campaign conducted to study the precipitation effects using the 73.5 GHz E-band terrestrial link in tropical areas. The results of one year of rainfall intensity and rain attenuation over three LOS terrestrial links in Malaysia are presented. The contributions of this paper can be summarized as follows:

- The rainfall rate was studied based on the rain precipitation data measured at every minute from three rain gauges installed along the experimental K and E-bands 1.8 km links. The empirical cumulative distribution of the 1-minute measured rain rate was compared with gamma and lognormal theoretical cumulative distribution models. The measured rain rate was also compared with several previous measurements and rain rate of ITU-R PN.837-1 [79] and ITU-R P.837-7 [80] prediction models.
- We investigated the rain attenuation along three experimental 73.5 GHz E-band and 21.8 GHz K-band links. Two for E-band links with the path length of 1.8 km and 300 m, and one K-band link of 1.8 km. The minimum received signal level (RSL) on a 15 minutes interval period was recorded by the link setup. The maximum rain attenuation was then computed by comparing the measured RSL during clear sky and rain conditions. The empirical cumulative distribution function (CDF) of the maximum rain attenuation was compared with the CDF of estimated 1-minute rain attenuation and with some prediction models such as ITU-R P.530-17 [81], and Mello [36] models. Comparison were also made between the results of the two 1.8 and 0.3 km E-band

TABLE 1. Rainfall intensity exceeded (mm/h) based on ITU-R P. 837-1 rain climatic zones.

Time Percentage (%)	A	B	C	D	E	F	G	H	J	K	L	M	N	P	Q
1.0	<0.1	0.5	0.7	2.1	0.6	1.7	3	2	8	1.5	2	4	5	12	24
0.3	0.8	2	2.8	4.5	2.4	4.5	7	4	13	4.2	7	11	15	34	49
0.1	2	3	5	8	6	8	12	10	20	12	15	22	35	65	72
0.03	5	6	9	13	12	15	20	18	28	23	33	40	65	105	96
0.01	8	12	15	19	22	28	30	32	35	42	60	63	95	145	115
0.003	14	21	26	29	41	54	45	55	45	70	105	95	140	200	142
0.001	22	32	42	42	70	78	65	83	55	100	150	120	180	250	170

links, as well as between the similar 1.8 km E-band and K-Band links.

- The results of the rain attenuation and the corresponding rainfall rate in this work were benchmarked with some previous studies conducted in different regions and at various E and K-band frequencies. The experimental data and the presented data analysis are useful to precisely quantify the influence of rain, and to improve the design and planning of mm-wave wireless communication systems in different regions.

The rest of the paper is organized as follows. Section III provides an overview of the rain rate. Section IV discusses the rain attenuation calculation and overview of several prediction models. Section V describes the measurement setup. Section VI explains the data processing. Section VII presents the rain rate statistical analysis, while Section VIII shows the rain attenuation statistical analysis. Section IX provides a comparison study for rain attenuation at K and E-bands for different experimental links around the world. Finally, Section X presents the conclusions.

III. RAIN RATE

The rainfall rate can be measured using different methods and instruments such as rain gauges and radars. The prominent and direct way to measure the rain rate is to use a rain gauge that measures the depth of water per unit of time [82]–[84]. The rain gauge and radar rainfall as an input of hydrological model were compared in tropical regions; i.e., Malaysia [85]. The Global Precipitation Measurement (GPM) Core Observatory (CO) spacecraft was designed to measure rain rates from 0.2 to 110 mm/h, detecting moderate to intense snow events [86]. In [87], the data sources and estimation methods of 30 currently available global precipitation data sets, including gauge-based, satellite-related, and reanalysis data sets were presented.

The rainfall events and rates vary among region, time and seasons [88]–[90]. Rainfall statistics near and above the Earth's surface are needed to estimate the percentage of absorption time or the dispersion of radio waves affecting the design of the radio system [91]. The rain rate distribution was modeled by a lognormal distribution at low rates and a gamma distribution at high rain rates [92]–[95]. This type of model was developed by Moupfouma *et al.* [18], [96] for both tropical and temperate climates. In certain situations, the exponential and generalized-Pareto PDFs can also be used to model the rain rate [97]. In [25], different distributions were examined for rainfall rate measurements over one year in Atsugi, Japan.

The International Telecommunication Union Radio Communication sector (ITU-R) has grouped the world into 15 rain climatic zones depending on the similarities of their rain characteristics, as shown in Table 1 [79]. According to time percentages and rain rate values in Table 1, the regions in Zones N, P and Q have high rainfall rates where Zone P is the highest. The ITU-R P.837-7 [80] presents a prediction method to calculate the rainfall rate exceeded for a desired average annual probability of exceedance and a given location on the surface of the Earth using digital maps of both monthly total rainfall and mean surface temperature. Tropical regions have a convective type of rainfall with high occurrence of rainfall events compared to temperate regions of the world [46], [55], [98]–[100].

IV. RAIN ATTENUATION

The rainfall rate has significant impact on radio propagation links, especially at mm-wave frequencies. The rainfall rate, operating frequency, link length, and type of polarization play crucial roles for designing the LOS terrestrial link. The impact of these factors on rain attenuation has been studied in [101]–[110]. Due to their impact on the rain attenuation, these factors are included in the ITU-R P.530-17 rain attenuation prediction model for terrestrial links [81]. Due to the strong relationship between rain attenuation and the rain rate, some studies have even used the attenuation of terrestrial links during the event of rain to estimate the rainfall rate [64], [68], [111]–[119].

Attenuation due to rain of any wireless communication link can be calculated from the distribution of specific attenuation along that link. The specific attenuation is obtained from the rain rate along the path using power law relationship [58], [120]–[122], and can be calculated per distance unit (dB/km) as [122]:

$$S_R = aR^b, \tag{1}$$

where a and b represent the regression factors which depend on several aspects such as the temperature, distribution of rain drop size, frequency and polarization [58]. The values of a and b can be experimentally obtained as empirical values. The ITU-R P. 838-3 [122] has the prediction values for a and b for 1-1000 GHz frequencies at vertical and horizontal polarization. The specific attenuation predictions for horizontal

polarization is higher than the vertical one for terrestrial paths, as reported in [123]. To simplify, the rain attenuation along the terrestrial link of d km can be calculated as the product of the specific attenuation with the path length of the link. This assumption is only valid if the rainfall rates are equally distributed along the path of the particular link. Considering the spatial inhomogeneity of the rain rate, the rain distribution is not uniform along the link, especially for long paths. Hence, the rain attenuation prediction models use the effective path length instead of actual path length to average out the spatial inhomogeneity of rain rate; thus, the specific attenuation. The rainfall rate is consider uniform in the effective path length. The effective path length is a product of correction factor with physical path length (L) of the link which can be defined as [81], [96]:

$$L_E = r \times L, \tag{2}$$

where r is the correction factor (reduction factor) which is usually less than unity except in rare cases [47]. It depends on the rain rate's spatial distribution and horizontal variation of rain along the link [39]. The direct method to obtain the rain attenuation for any terrestrial link is the radio propagation measurement. The measured rain attenuation is simply calculated from RSL by determining the amount of signal degradation during rain conditions compared to the amount of RSL in the clear sky condition. It can be calculated as [72]:

$$RA(\text{dB}) = RSL_{\text{clear sky}} - RSL_{\text{rain}} \tag{3}$$

The rain attenuation based on (3) may cause overestimation due to the wet antenna effect after rain occurrence. To overcome the wet antenna effect, the antenna radome can be covered with an additional hydrophobic material [5], [124]. The wet antenna attenuation can also be calculated and excluded from the rain attenuation of (3). Some studies have investigated the wet antenna effects on terrestrial links at different microwave and mm-wave frequencies [125]–[134]. In this work, the acrylonitrile styrene acrylate (ASA) was used as the antenna's radomes. ASA has great toughness and rigidity, good chemical resistance, thermal stability, and outstanding weather resistance [135]. The antenna's radomes wet attenuation is calculated from the difference between the RSL in the clear sky condition period to the RSL during the first hour after the rainfall has stopped. Based on our measurement over a one-year period, the average antenna's radomes wet attenuation is 1.5 dB. This value is similar to the wet antenna attenuation calculated in [124], [132]. This value is excluded from the measured rain attenuation.

Using long-term rainfall rate statistics, the rain attenuation can be predicted. The simple form for rain attenuation prediction at percentage time of p (A_p) is:

$$A_p(\text{dB}) = S_{R_p} \times L_E \quad , \tag{4}$$

where S_{R_p} is the specific attenuation (dB/km is defined in (1) for the rainfall rate R_p (mm/h) exceeded at p% of time and L_E is the effective path defined in (2). By substituting (1) and (2) in (4), the general formula for rain attenuation can be defined as:

$$A_p(\text{dB}) = aR_p^b \times r \times L \tag{5}$$

The descriptions for several well-established rain attenuation models based on (5) with different reduction factor values are presented as follows.

A. LIN MODEL

The rain attenuation model in [136] was proposed by Lin based on long-term rain rate statistics and empirical rain attenuation fitting from the measurement data at 11 GHz. The reduction factor of this model accounts for partially correlated rain rate variations along the propagation path length. The reduction factor of this model is defined as:

$$r = \frac{1}{1 + L/\bar{L}(R_p)}, \tag{6}$$

where $\bar{L}(R_p)$ is the characteristic path length that can be computed using $(\bar{L}(R_p) \approx \frac{2636}{R_p - 6.2})$ for R_p> 10 mm/h . $\bar{L}$ is related to the diameter of the rain cell such that the reduction factor is equal to half when $\bar{L} = L$. Next, the rain attenuation is calculated based on (5) for the rainfall rate exceeded at p% of time.

B. ITU-R P.530-17

The ITU-R P.530-17 [81] is the latest ITU-R recommendation for terrestrial LOS link propagation and prediction methods. It recommends calculating the rain attenuation ($A_{0.01}$) for the rainfall rate using (5). Next, the rain attenuation (A_p) for other rainfall rates is computed by scaling $A_{0.01}$ to other percentages of time p%. The r reduction factor in (5) is calculated as:

$$r = \frac{1}{0.477L^{0.633}R_{0.01}^{0.073b}f^{0.123} - 10.579(1 - e^{-0.024L})} \tag{7}$$

where f is the frequency in GHz and the maximum recommended r is 2.5 [81]. The attenuation exceeding other percentages of time p in the range of 0.001%–1% of the year A_p(dB) can be calculated as follows:

$$A_p = A_{0.01}c_1 p^{-(c_2 + c_3 \log_{10} p)}, \tag{8}$$

where

$$\begin{aligned} c_0 &= 0.12 + 0.4\log_{10}(f/10)^{0.8} \\ c_1 &= 0.07^{c_0}(0.12^{1-c_0}) \\ c_2 &= 0.855c_0 + 0.546(1 - c_0) \\ c_3 &= 0.139c_0 + 0.043(1 - c_0) \end{aligned} \tag{9}$$

C. MOUPFOUMA MODEL

The Moupfouma model in [22] and [137] is based on the rainfall rate exceeded at 0.01% of the time. The details of rain attenuation (A_p) determination for other rainfall rates can be found in [22]. When adopting this model, the $A_{0.01}$

rain attenuation is calculated using (5) at the rainfall rate of $R_{0.01}$ mm/h, where the r value is computed using:

$$r = exp(\frac{-R_{0.01}}{1 + \zeta(L) \times R_{0.01}}), \tag{10}$$

where

$$\zeta(L) = -100, \quad for \ \ L \leq 7\ km$$
$$\zeta(L) = (\frac{44.2}{L})^{0.78}, \quad for \ \ L > 7km$$

D. SILVA MELLO MODEL

The Silva Mello model [14], [36] uses the rain rate distribution R_p to correct the underestimation of the attenuation predicted by the ITUR model, especially in low latitude areas with serious precipitation regimes. By incorporating two variables (the effective rain rate (R_{eff}) in specific attenuation and the rain cell diameter (d_0)), the rain attenuation (A_p) exceeded at $p\%$ percentage of time is calculated as:

$$A_p(\text{dB}) = a(R_{eff})^b \times \frac{1}{1 + \frac{L}{d_0(R_p))}} \ , \tag{11}$$

where

$$R_{eff} = 1.763R^{0.753+0.197/d}$$
$$d_0 = 119R^{-0.244}$$

V. EXPERIMENTAL SETUP

The rain rate and rain attenuation measurement setups and test bed environment are extensively discussed as follows.

A. RAIN ATTENUATION MEASUREMENT

The transmitter (Tx) and receiver (Rx) equipment for K and E-bands for this measurement campaign are manufactured by Ericsson, i.e. the Mini Links ML-6363 and ML-6352. The specification details of the ML-6363 and ML-6352 are provided in [138], [139]. The 21.8 GHz K-band and 73.5 GHz E-band link setups have been operated from September 2018 to study the effect of rain. The 21.8 GHz link is tuned to support up to 225 Mbps by using a bandwidth of 28 MHz channel and adaptive modulation of up to 1024 QAM. The 73.5 GHz link is tuned to support up to 4.532 Gbps by using a bandwidth of 750 MHz channel and adaptive modulation of up to 256 QAM. The parameters for the measurement setup for both links, including the antenna specifications, are provided in Table 2, where both Tx and Rx at each link adopted similar antenna specifications. The data loggers at Rx recorded the maximum and minimum RSL values every 15 minutes. Both links are located in Universiti Teknologi Malaysia (UTM), Kuala Lumpur (KL), Malaysia, with radio propagation LOS path length of 1.8 km. The Tx for both links, labeled Site A (3°11'7''N, 101°43'46''E), are located at the top of a 5-storey student residential building (49 m above sea level) outside the university campus. The Rx for both links, labeled Site B (3°10'21''N, 101°43'10''E), are located on a level 16 in one of the high-rise management building (43 m above sea level) at the university campus.

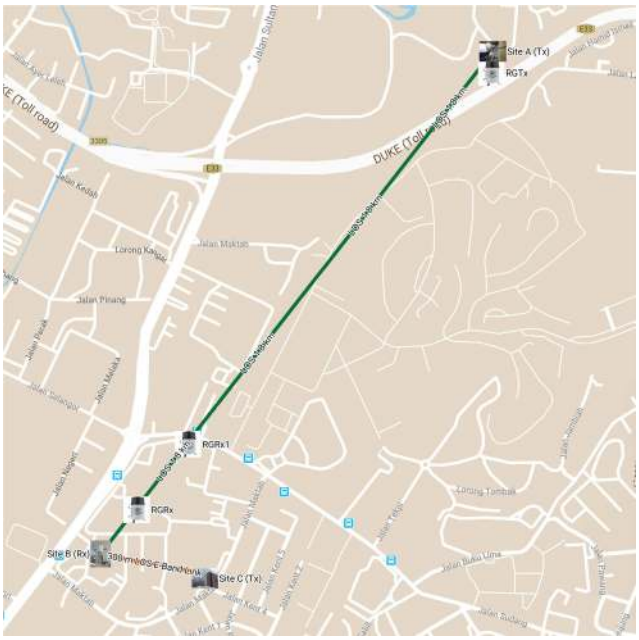

FIGURE 1. Measurement links map in Kuala Lumpur, Malaysia for 1.8 km LOS path at K and E-bnads between Kolej Siswa Jaya (Tx site) and Menara Razak, Universiti Teknologi Malaysia (Rx site), and 300 m LOS path at E-band between Kolej Siswa Jaya (Tx site) and Residensi UTM (Rx Site).

Another E-band link has been established inside UTM, KL campus where the measurement setup parameters are listed in Table 2. The Rx is located on Site B while the Tx, labelled as Site C (300 m LOS from Site B) (3°10'20''N, 101°43'19''E), is located at the rooftop of Residensi UTM building (41 m above sea level). Figure 1 presents the map of the measurement setup and the pictorial view at Tx and Rx sites.

B. RAIN RATE MEASUREMENT

To collect the rainfall rate along the route of the three link setups (discussed in Section V-A), three HOBO data logging rain gauges have been installed in the link paths. The data logging rain gauge system is battery powered and includes data logger with a tipping-bucket rain gauge of 0.2 mm sensitivity. Details on the rain gauge specifications are given in [140]. Two rain gauges were installed at the Rx site while the third was installed at the Tx site, as shown in Figure 1. The two Rx rain gauges (named RGRx and RGRx1) were located at the rooftops in two different buildings separated about 130 m and 380 m from the Rx, respectively. The Tx rain gauge (RGTx) was located at the rooftop of the building near the Tx building (about 50 m from Tx antenna). The rain gauges record the rainfall that occurs every minute; i.e., at an integral multiple of 12 mm/h.

VI. POST PROCESSING OF RAIN RATE AND RAIN ATTENUATION DATA

This section discusses the details of the post processing used on the data collected from the rain gauges, and from the

TABLE 2. Parameters of experimental terrestrial links.

Descriptions	K-Band 1.8 km	E-Band 1.8 km	E-Band 300 m
Transceiver Name and Manufactured	Mini Links ML-6363,Ericsson	Mini Links ML-6352,Ericsson	Mini Links ML-6352,Ericsson
Frequency	21.8 GHz	73.5 GHz	73.5 GHz
Bandwidth	28 MHz	750 MHz	750 MHz
Antenna Type	Directional 0.6 m (ANT3 0.6 23 HP)	Directional 0.3 m (ANT2 0.3 80 HP)	Directional 0.2 m (ANT2 0.2 80 HP)
Polarization	Vertical	Vertical	Vertical
Antenna Gain	40.7 dBi	46.5 dBi	43.5 dBi
Antenna HPBW	1.7°	0.8°	1.1°
Max Tx Power	20 dBm	15 dBm	15 dBm
10^{-6} BER Received Threshold	-79 dBm	-75 dBm	-75 dBm

E and K-bands' Mini Links for the purpose of statistical analysis. The minimum RSL at the Rx has been recorded every 15 minutes and the rain attenuation is calculated based on (3). Here, the $\text{RSL}_{\text{clear sky}}$ is the minimum RSL during the clear sky condition and the RSL_{rain} is the minimum RSL during rain condition. The reference level of the received signal can be calculated from the averaged RSL just before and after rain occurrence [141]. In this work, the average of all recorded minimum $\text{RSL}_{\text{clear sky}}$ during the measurement period is used as a reference signal level (RL). Some algorithms have been proposed in [142]–[144] to enhance the accuracy of choosing the RL. Here, the maximum rain attenuation is calculated as:

$$RA_{\max}(\text{dB}) = RL - RSL_{\text{minimum during rain}} \tag{12}$$

The rainfall rate has been recorded at one minute intervals. To correlate the rain rate data with the maximum rain attenuation ($\text{RA}_{\max}$), the maximum rain rate of 15-minute intervals is calculated. From the data processing of the minimum RSL and maximum rain rate every 15 minutes along the year, we noticed that the average antenna wet attenuation along the year is 1.5 dB. The wet antenna attenuation is calculated from the difference between the average RSL during the clear sky condition and the RSL after 15 to 60 minutes of rain condition. We used the maximum measured 15-minute interval rain as an indicator that the rain has stopped. In some cases, the rain rate data is zero but the RSL is more than the average RSL of clear sky condition by 0.5 to 2.4 dB with the average of 1.5 dB (indicating the wet antenna effect).

For the post-processing of the rain rate data, collected from three rain gauges along the path link, the rain rate at each location along the communication path is estimated by using the inverse distance weighting (IDW) method [145]. IDW has been effectively used as one of the standard spatial interpolation procedures [146], [147]. Using the IDW procedure, the estimated value R_p is a weighted sum of the rain gauge values R_i given by:

$$R_p = \sum_{i=1}^{N} w_i R_i \tag{13}$$

where $N = 3$ in this case (i.e., the number of rain gauges). The weight of each rain gauge value w_i on the estimated location p depends on the distance d_i in between, and is given by [148], [149] as:

$$w_i = \frac{d_i^{-2}}{\sum_{i=1}^{N} d_i^{-2}} \tag{14}$$

The average rain rate is then calculated from these estimated values (named RGE), together with the rain gauge readings, and is used in this study.

The standard deviation of the maximum rain attenuation (σ_{RA}) is calculated based on mean values of the maximum rain rate (μ_R) as follows. The maximum rain rates for every 15 minutes of RGE are grouped to multiples of 12 ($R = 12$, 24, 36,….mm/h). Let R represent the vector that contains all rain rate data and R_i is the rain rate data for group i, where $R_i \subset R$ ($i = 1, 2, \ldots, N$) contains the values R_{ie} defined as:

$$\begin{aligned} R_{ie} &\le 12, \quad \text{for } i = 1 \\ 12(i-1) < R_{ie} &\le 12i, \quad \text{for } i = 2, 3, \ldots, N \end{aligned}$$

The values of rain rate at each group are averaged out to obtain the mean of rain rate $\overline{R_i}$ and its corresponding mean maximum rain attenuation $\overline{RA_i}$. Next, we calculated the standard deviation σ_{RA} of the corresponding values of the maximum rain attenuation due to the rainfall rate of each group. The σ_{RA} is defined as:

$$\sigma_{RA_i} = \sqrt{\frac{\sum_{e=1}^{M} (RA_e - \overline{RA_i})^2}{M-1}}, \tag{15}$$

where M is the number of rain attenuation observation values in group i, which varies among groups 1 to N.

VII. STATISTICAL ANALYSIS OF RAIN RATE

The rainfall rate measurements were collected in tropical region for one year, from 6th September 2018 until 5th September 2019, using three different rain gauges on the link path, as described in Section V-B. Based on the annual reports of the Malaysian Meteorological Services (MMS) in 1987, there are three categories of rainfall in tropical regions: thunderstorm, shower, and drizzle [46], [103]. The thunderstorm rainfall rate is more than 70 mm/h, and the shower rainfall rate is in the range of 20-70 mm/h. The rainfall rate of drizzle is less than 20 mm/h. More details on rain categories in tropical region are found in [46].

Figure 2 shows the cumulative distribution function (CDF) of the measured rainfall rate along the link. Four curves

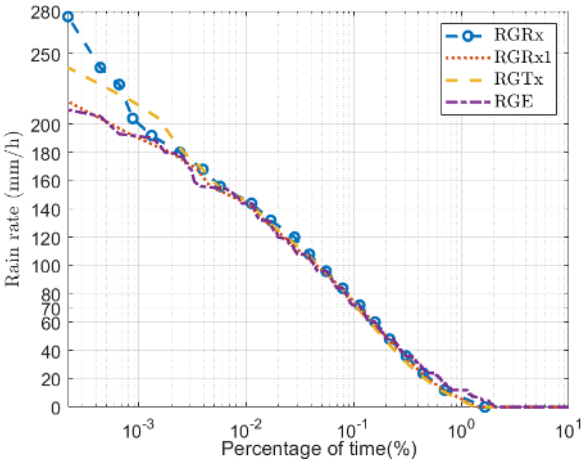

FIGURE 2. Cumulative distribution for the measured rain rate per minute.

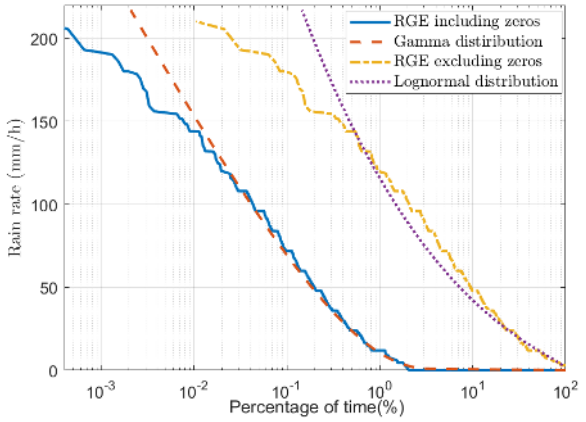

FIGURE 3. Cumulative distribution for the measured rain rate using RGE compared to some theoretical cumulative distribution models.

(legends as RGRx, RGRx1, RGTx, and RGE) present the measurement of the rain rate along the experimental link. It is clear that the CDFs for the measured rain rate from RGRx, RGRx1, RGTx, and the estimated RGE using (13) are very close to each other at percentage of time larger than 0.01%. However, there are few differences between them in the percentage of time lower than 0.01%. Figure 2 shows that the best agreement is between the measured rain rate of RGRx1 and the estimated rain rate from three rain gauges (RGE). Figure 3 displays the CDF for RGE compared to the lognormal and gamma distribution models. It can be shown that the gamma distribution model fits the RGE rainfall rate data well at 0.02% of time and above (rain rate is $\leq$ 120 mm/h) and has slight deviation at the rain rate above 120 mm/h. It is also shown that the deviation is larger for high rain rate of 150 mm/h and above. For lognormal distribution, the data with rainfall rate of zero value were excluded. The lognormal distribution is comparable with RGE measured data at 0.5% of time and above, and agrees well with RGE at 20% of time and above (low rainfall rate $\leq$ 26 mm/h).

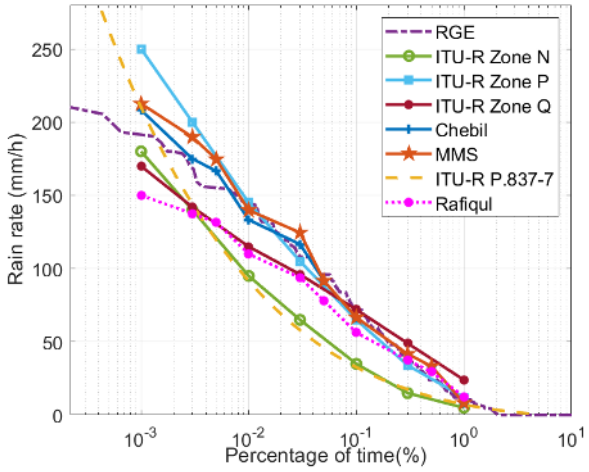

FIGURE 4. Cumulative distribution for the measured rain comparing with ITU-R Models and some previous measurements.

According to the ITU-R rain Zones in Table 1, Malaysia falls in Zone P. The CDF of the measured rainfall rates is compared with the ITU-R Zones N, P, and Q at time percentage p% for p from 0.001 to 1. The experimental CFD is also compared with rainfall of 1-hour integration time data collected from the Malaysian Meteorological Station (MMS) over 12 years [150]. Chebil and Rahman's model [150] was used to convert the rain rate data to the equivalent 1-minute integration time.

A total of eight curves are plotted in Figure 4 to present the cumulative distributions of the rain rates. The measured rain rate of RGE at 0.01% of 144 mm/h is equal to the predicted rain rate by the ITU-R Zone P of 145 mm/h, which is only less by 1 mm/h. It is also close to the ITU-R Zone P at the percentage of time ($p \geq 0.01$%). The measured rain rate using RGE at 0.1% is equal to the predicted value by ITU-R Zone Q. At the time percentage of 0.001%, the predicted rain rate by ITU-R Zone N is close to the measured rain rates of RGE with slight underestimation by 10 to 12 mm/h. However, the ITU-R Zone P predicted value of 250 mm/h at 0.001% had overestimated the RGE measurement value by 58 mm/h.

The measurements of rainfall rate are also compared with the latest ITU-R P.837 series [80]. Figure 4 shows that the rain rates of ITU-R P.837-7 model [80] are comparable with measured rain rates in the high percentage of time 1% and above (low rain rates below 12 mm/h). At the time percentage of 0.6% to 0.002%, the ITU-R P. 837-7 rain rates are underestimated when compared to our measured rain rates. At 0.01% of time, the ITU-R P.837-7 rain rate is 92 mm/h, however, the rain rates of measurement are 146, 144, 146, and 144 mm/h for RGRx, RGRx1, RGTx, and RGE, respectively. This implies that the ITU-R P.837-7 model at 0.01% had underestimated our measured rain rate by 52 to 54 mm/h and the predicted rain rate of ITU-R PN.837-1 Zone P by 53 mm/h. It is noted that the rain rates of ITU-R P.837-7 and ITU-R PN.837-1 Zone N models are very close at the percentage of time of 0.003% and above.

Figure 4 also shows a comparison between our measurement, and the rain rate data from MMS, and the measurement conducted by Chebil et.al. [150] over three years, from June 1992 to May 1995 at 3°08'N, 101°39'E, located within the region of RGRx1. Figure 4 also shows the comparison with the average of conducted rain rate measurement by Rafiqul et.al. [90] over 6 years form 2011 to 2016 at 3.2505°N, 101.7347°E (about 10 km from our experiment). It can be seen that the MMS and Chebil rain rate data are very close to the rain rate measurement of RGE at the percentage of time ($p \geq 0.01\%$). The rain rates of Rafiqul's measurement are very close to our measurement of RGE at the rain rate of 0.05% of time and above. At 0.03% to 0.003% of time, Rafiqul's rain rate measurements are in the best agreement with the rain rate of ITU-R Zone Q. The rain rates of Rafiqul are also very close to the ITU-R Zone Q at 0.003% to 0.001%. From the MMS, Chebil, Rafiqul, and our measurements, it can be concluded that the rain climate in the city of Kuala Lumpur, Malaysia falls in the rain region of ITU-R Zones P and Q.

VIII. STATISTICAL ANALYSIS OF RAIN ATTENUATION

In this section, the rain attenuation's statistical analysis for two E-band links and one K-band link are discussed. All results in the following subsections are based on post processing, as discussed in Section VI. Here, our rain attenuation and rain rate results refer to the maximum rain attenuation corresponding to the maximum rain rate per 15 minutes.

A. RAIN ATTENUATION AT E-BAND

Figures 5a and 5b show the CDF of the maximum measured rain attenuation for two links: 73.5 GHz E-band and their corresponding maximum rain rates. For the 1.8 km E-band link, the maximum rain attenuation is 40.1 dB at 0.03% of time and the maximum rain rate is 108 mm/h, as presented in Figure 5a. Figure 5b shows that the maximum rain attenuation for 300 m link is 25 dB at 0.006% of time with the maximum rain rate of 193 mm/h. It means that the outage probabilities are around 2.9×10^{-4} and 5.9×10^{-5} for 1.8 km and 300 m E-band links, respectively. In Figure 5a, the line curve for the rain attenuation of 1.8 km shows no changes in rain attenuation values after 40 dB. This implies that the reading of RSL by Rx is the receiver sensitivity and the actual RSL is below the Rx threshold. In other words, the 1.8 km link is down when the rain attenuation is more than 40 dB, and occurs when the rain rate is above 108 mm/h. In contrast, the 300 m link has rain attenuation around 13 dB when the maximum rain rate is 108 mm/h, as depicted in Figure 5b. The 300 m link is down only when the maximum rain rate is above 193 mm/h.

The maximum rain attenuation along one year of measurements for the 1.8 km and 300 m based on the measured rain rate of RGE, RGRx, RGRx, and RGTx is shown in Figures 6a, b, c, and d, respectively. Using the classification of rainfall types, as discussed in Section VII, the maximum rain attenuation at 1.8 km and 300 m links for each rainfall class is shown in Figures 7(a-c). The rain attenuation at

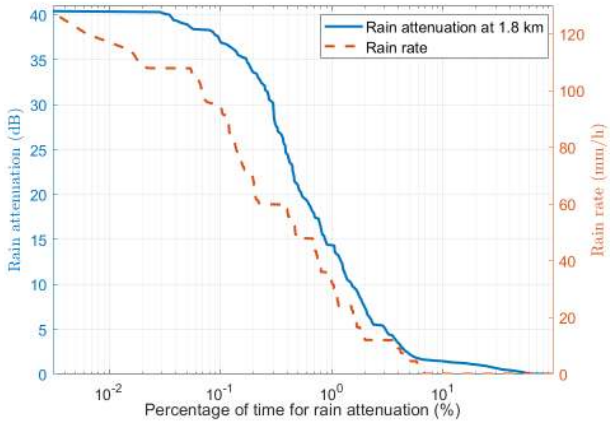

(a) CDF of 1.8 km E-band link

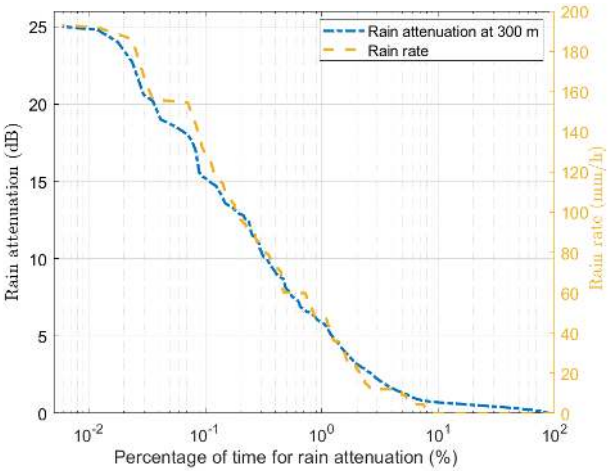

(b) CDF of 300 m E-band link

FIGURE 5. Cumulative distribution for the maximum rain attenuation at E-band links with maximum rain rate (a) 1.8 km link and (b) 300 m link.

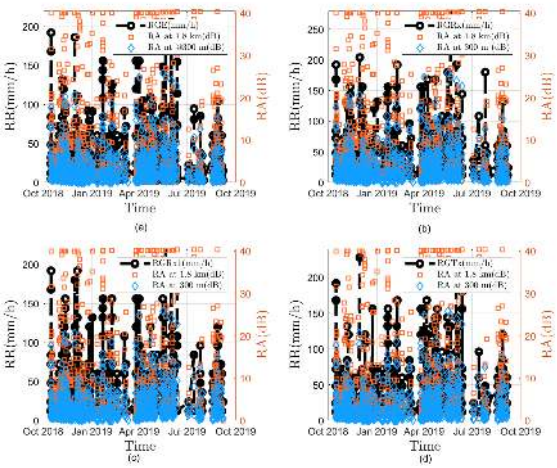

FIGURE 6. Maximum rain attenuation for 1.8 and 0.3 km links at the maximum rain rate using (a) RGE, (b) RGRx, (c) RGRx1, and (d) RGTx.

corresponding drizzle rainfall (0-20 mm/h rain rates) is shown in Figure 7. It can be seen that the rain attenuation values along the year for 300 m link are below 10.2 dB, and most

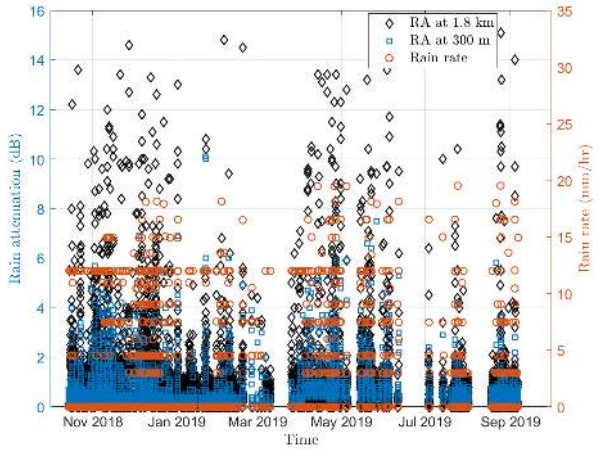

(a) RA at drizzle rain

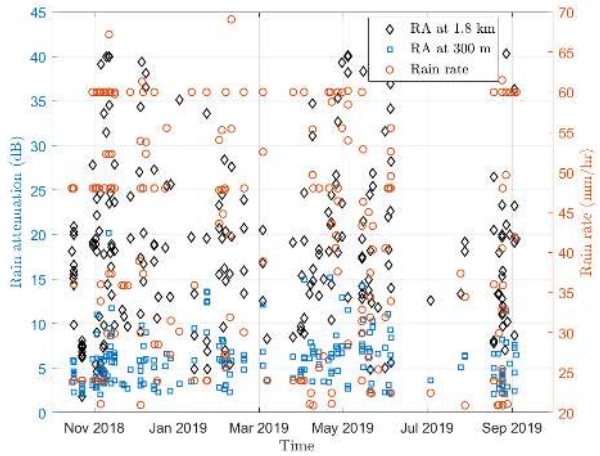

(b) RA at shower rain

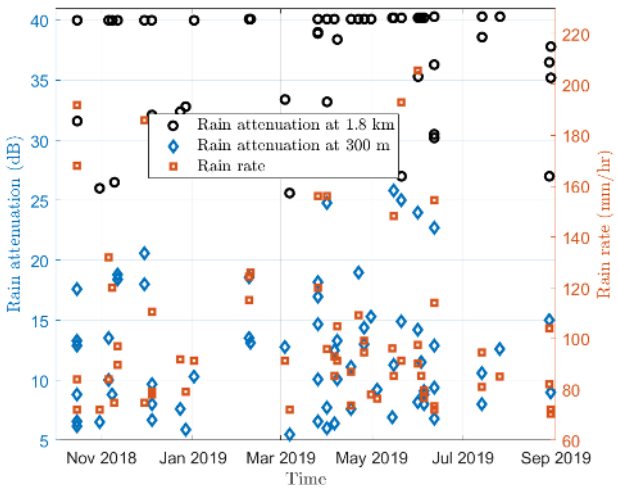

(c) RA at thunderstorm rain

FIGURE 7. Comparison of the maximum rain attenuation at 1.8 and 0.3 km links for three rainfall types (a) Drizzle (b) Shower and (c) Thunderstorm.

of the values are below 4 dB at drizzle rainfall type. The rain attenuation values along the year for 1.8 km are below 15.2 dB with many recorded values above 6 dB. For shower

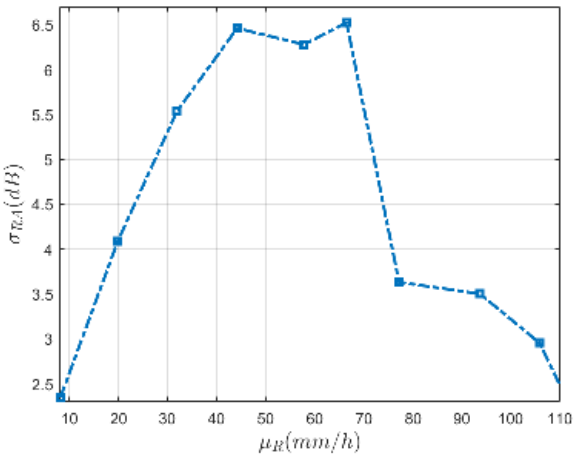

FIGURE 8. Standard deviation of the maximum attenuation according to mean values of maximum rain rate in one year for 1.8 km link of 73.5 GHz E-band.

rainfall (20-70 mm/h rain rate), the rain attenuation for all months is less than 20.3 and 40.1 dB for 300 m and 1.8 km, respectively, as shown in Figure 7b. The rain attenuation for 1.8 km link reaches the maximum rain attenuation value at shower rainfall, however, most of values along the year are below 25 dB; and for the 300 m link, below 15 dB. The rain attenuation for thunderstorm rainfall is the maximum among all rainfall types, as shown in Figure 7c . It can be seen that the rain attenuation is more than 5 and 25 dB along the year for this type of rainfall for of 300 m and 1.8 km, respectively. Figures 7(a-c) also show the dispersion of rain attenuation at the corresponding rainfall rate. It is more along the 1.8 km link in the shower rainfall category, as shown in Figure 7b.

To further assess the dispersion of rain attenuation, the standard deviation of the maximum rain attenuation (σ_{RA}) is calculated using (15), as discussed in Section VI. Figure 8 shows that the σ_{RA} varies from 2.3 to 6.5 in the range of μ_R of maximum rain rate from 8.1 mm/h to 110 mm/h. The maximum dispersion of rain attenuation occurs with the range of σ_{RA} from 5 to 6.5 for the μ_R maximum rain rate of 31 mm/h to 70 mm/h. This implies that the high rain rates correspond to small rain cell size and low rain rates have greater drop size distribution variability.

Based on ITU-R rain climate Zones in Table 1, Zones N, Q, and P are classified as zones with high rainfall rate and Zone P the highest among them, as discussed in Section III. Here, the ITU-R P.530-17 is used to calculate the rain attenuation based on the rain rate at 0.01% of time (R_{001}). The ten curves plotted in Figure 9 show the CDFs of the maximum measured rain attenuation every 15 minutes (maximum measured) for 1.8 km and 300 m links compared to the calculated rain attenuation every minute using ITU-R P.530-17 prediction model. The R_{001} values of ITU-R Zones N, P, Q (95, 145, 115 mm/h), and the R_{001} of measurement rainfall rate (144 mm/h), legend as Estimated/min, are used in ITU-R P. 530-17 prediction model for rain attenuation calculation. Figure 9 shows that at the percentage of time range from 0.03-1%, our

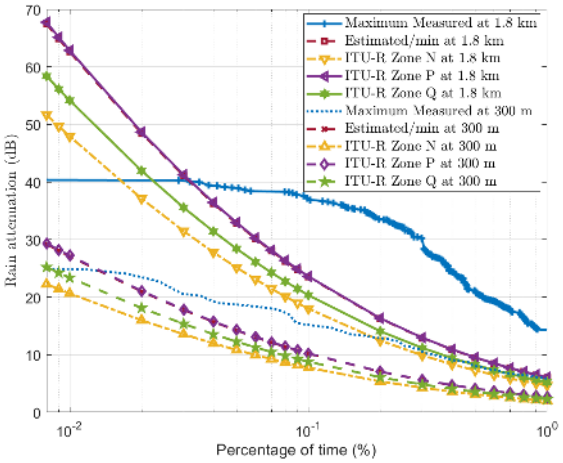

FIGURE 9. Cumulative distribution for the maximum rain attenuation at 1.8 km link and 300 m link compared to predicted rain attenuation using ITU-R P.530-17 model.

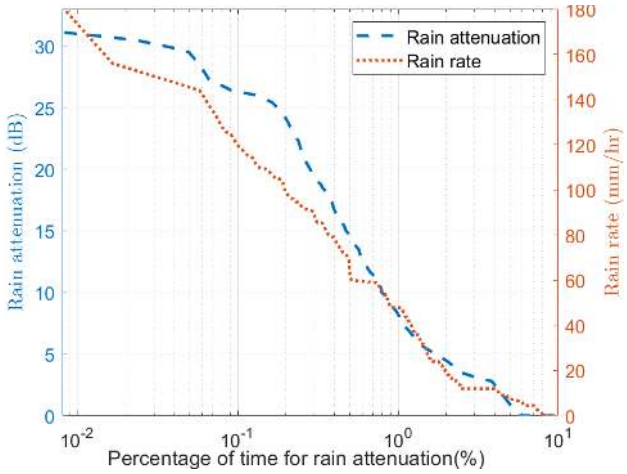

FIGURE 10. Cumulative distribution for the maximum rain attenuation and maximum rain rate at 21.8 GHz K-band link.

measured rain attenuation varies between 40.1 to 14.3 dB and 20.4 to 5.9 dB for 1.8 km and 300 m links, respectively. It is shown that the Estimated/min at 1.8 km and at 300 m predicted rain attenuation values completely match with the attenuation of ITU-R Zone P at 1.8 km and 300 m links, respectively.

Since the attenuation per minute must be equal or less than the maximum attenuation per 15 minutes, from visual inspection of Figure 9, we can see that the ITU-R model over estimates the attenuation that exceeds 0.03% of the year for 1.8 km link. The attenuation for other percentages of time (from 0.04 to 1% of the year) for 1.8 km, as well as at percentages of time from 0.01 to 1% for 300 m link, are below the maximum attenuation per 15 minutes.

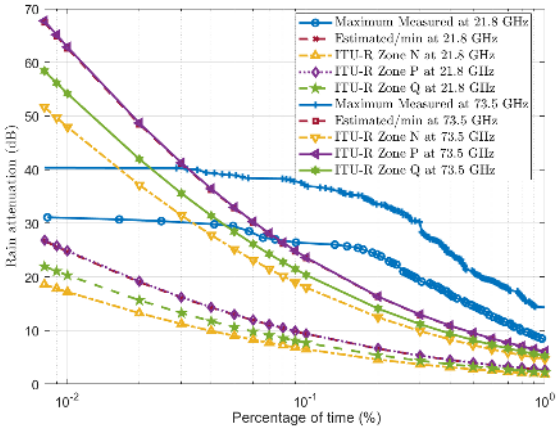

FIGURE 11. Cumulative distribution for maximum rain attenuation at 1.8 km for 21.8 and 73.5 GHz compared to predicted rain attenuation using ITU-R P.530-17 model.

B. RAIN ATTENUATION AT K-BAND

In this section, the results for rain attenuation at 21.8 GHz K-band are discussed and compared with the E-band. Both the K-band and E-band links were established in the same sites with a link distance of 1.8 km. Figure 10 shows the CDF of maximum rain attenuation for 21.8 GHz along 1.8 km distance and its corresponding maximum rain rate. It can be seen that the rain attenuation varies between 2.8 to 31.1 dB at the percentages of time 3.9-0.008% corresponding to the maximum rain rate of 12-180 mm/h. It is noted that the K-band link of 1.8 km is down when the maximum rain rate is above 180 mm/h. As compared to the same 1.8 km LOS link using the E-band of 73.5 GHz, it can be concluded that the maximum rainfall threshold of 21.8 GHz K-band and 73.5 GHz E-band are 180 and 108 mm/h, respectively. In particular application, based on the configuration of these links and the results of rain attenuation, the E-band link that can support high capacity can be used for clear sky condition and rainy condition with rain rates below 108 mm/h. For any rain rate above 108 mm/h, the particular application can be provided with capacity sacrifice using the K-band link of 21.8 GHz.

Figure 11 shows the maximum measured rain attenuation CDF every 15 minutes for 21.8 and 73.5 GHz 1.8 km links as well as the calculated rain attenuation every minute using ITU-R P.530-17 prediction model. The R_{001} values of ITU-R Zones N, P, Q (95, 145, 115 mm/h) and the R_{001} from our measurement rainfall rate (144 mm/h), legend as Estimated/min, are used in ITU-R P. 530-17 prediction model for rain attenuation calculation. Figure 11 shows that, from the measured and predicted rain attenuation, the rain attenuation of 73.5 GHz is slightly more than the rain attenuation of 21.8 GHz at the high percentage of time (low rainfall rate). The difference becomes larger at the low percentage of time (high rainfall rate). At 1% of time (low rain rate), from our measurement, the rain attenuation at 73.5 GHz is around 5 dB higher than 21.8 GHz, however, at 0.03% of time (high rain rate) the difference is 10 dB. For the predicted rain attenuation using ITU-R (i.e. the rain attenuation of ITU-R Zone P

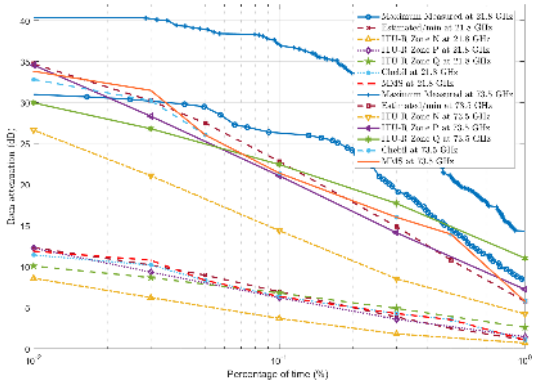

FIGURE 12. Cumulative distribution for maximum rain attenuation at 1.8 km for 21.8 and 73.5 GHz compared to predicted rain attenuation using the Mello model.

of 73.5 GHz) is greater than the corresponding 21.8 GHz by 3.5 and 25 dB at 1% and 0.03% of time, respectively. It is also shown that the Estimated/min at 21.8 GHz and at 73.5 GHz predicted rain attenuation values completely match with the attenuation of ITU-R Zone P at 21.8 and 73.5 GHz of 1.8 km link, respectively.

Using our rainfall rate measurement (legend as Estimated/min), Chebil measurement, MMS measurement, and the predicted one using ITU-R at Zones N, P, and Q, the rain attenuation at 21.8 and 73.5 GHz for 1.8 km link is calculated using the Silva Mello model (explained in Section IV-D) and the results are presented in Figure 12. The predicted rain attenuation per minute for both K and E -bands are less than the maximum rain attenuation per 15 minutes at all percentages of time. From the visual inspection of Figure 12, it is noted that the predicted curves of rain attenuation for all measured rainfall (Estimated/min, Chebli, and MMS) is comparable with the the predicted curves of rain attenuation based on the rainfall rate of ITU-R Zones P and Q at most of percentages of time for both 21.8 and 73.5 GHz bands. The predicted rain attenuation based on the rainfall rate of ITU-R Zone N is underestimated compared to those with high deviation at 73.5 GHz.

IX. COMPARISON STUDY OF RAIN ATTENUATION AT K AND E-BANDS AT DIFFERENT REGIONS AROUND THE WORLD

In this section, the rain attenuation at K and E-bands for different regions in the world are discussed and compared. Table 3 presents the comparison of several previous studies of rain attenuation at K-band in different regions. The rain attenuation at 18 GHz band was analyzed in South Korea and Brazil. Based on three years rainfall rate measurements at South Korea, the rain rate values are 50 and 100 mm/h at the time percentage of 0.01% and 0.001%, respectively [66], [67]. The corresponding rain attenuation values for 50 mm/h along 3.2 km link are 33.38 and 21.88 dB for horizontal and vertical polarizations, respectively. At 0.001% of time (rain rate of 100 mm/h), the rain attenuation values are 43.5 and 38.5 dB for horizontal and vertical polarizations, respectively. The link experiences more rain attenuation at horizontal polarization. In [31]–[33], the rain attenuation for the same band of 18 GHz in Brazil is 33 dB along 7.5 km vertical polarization link at 0.001% of time (120 mm/h rain rate). The rain rate at 0.01% of time (50 mm/h) is extremely high at South Korea compared to the rain rate of 6 mm/h at 0.01% of time in Brazil.

The rain attenuation at 26 GHz was studied in Prague, Czech Republic and Malaysia. In Prague, the rain attenuation over 4 years of measurements along 5.5 km link varies between 20 to 35 dB and 17 to 31 dB at 0.01% of time (20-60 mm/h rain rates) for horizontal and vertical polarizations, respectively [65]. In Johor Bahru, Malaysia [51], [52], at the same percentage of time 0.01%, the rain rate of 120 mm/h is twice the rain rate in Prague, Czech Republic. The rain attenuation at 26 GHz in Malaysia is 34 dB at 0.01% of time along 1.3 km horizontal polarization link.

The rain attenuation at 19.5 GHz was studied over one year along 6.73 km horizontal polarization link in Durban, South Africa [62], [63]. The rain attenuation is 25 dB at 0.01% of time with rain rate less than 80 mm/h. Based on the statistics of rain attenuation in Singapore [55] at 21 GHz along 10 years over 1.1 km, the rain attenuation values among 120 mm/h rain rate are 22 and 27.5 dB for vertical and horizontal polarizations, respectively. In our work, the rain attenuation at 21.8 GHz among 120 mm/h along 1.8 km link (vertical polarization) is 26.4 dB. Our rain attenuation at 21.8 GHz K-band is comparable to the rain attenuation at 21 GHz K-band in Singapore [55].

Table 3 displays three different measurements at K-band at different frequencies in Malaysia including this work. The rainfall rate has some differences for both percentages of time 0.01% and 0.001%. The rational of these variances is the difference of geographic area of the measurement and the time. In [40] and [51], the measurements were conducted at the same area in Universiti Teknologi Malaysia (UTM), Skudai in different years; 1999 and 2011 to 2012, respectively. In [40], the rainfall rates are 127 and 185 mm/h for 0.01% and 0.001% percentages of time, respectively. However, in [51], the rainfall rates are 120 and 168 mm/h for 0.01% and 0.001% percentages of time, respectively. The rain rates based on measurements in 1999 [40] are more than the rain rates in May 2011 to Jun 2012 [51] by 7 and 17 mm/h for 0.01% and 0.001% percentages of time, respectively. Here, the measurements were conducted at different locations and time, as discussed in SectionV. The rain rates in this experiment are 144 and 193 mm/h for 0.01% and 0.001% percentages of time, respectively. It is more than the one conducted in [51] by 22 and 24 for 0.01% and 0.001% percentages of time, respectively. In [40], the rain attenuation for 0.3 km horizontal polarization link at 23 GHz is 17 and 25 dB at the time percentages of 0.01% and 0.001%, respectively. The rain attenuation at 26 GHz is 34 and 50 dB at the time percentages of 0.01% and 0.001%, respectively [51].

TABLE 3. Comparison of different rain attenuation studies at K-band.

Source	Region	Frequency (GHz)	Period (Year)	Polarization	Distance (km)	Rain Rate (mm/h)	Rain Attenuation (dB)	Time Percentage (%)
[66], [67]	South Korea	18.0	3	Horizontal, Vertical	3.2	50 100	33.38,21.88 43.50,38.50	0.01 0.001
[65]	Prague	26.0	4	Horizontal, Vertical	5.5	20-60 60-100	20.00-35.00,17.00-31.00 39.00,34.00	0.01 0.001
[31]–[33]	Brazil	18.0	1	Vertical	7.5	6 120	- 33.00	0.01 0.001
[62], [63]	South Africa	19.5	1	Horizontal	6.7	80	25.00	0.01
[40]	Malaysia	23.0	1	Horizontal	0.3	127 185	17.00 25.00	0.01 0.001
[51]	Malaysia	26.0	1	Horizontal	1.3	120 168	34.00 50.00	0.01 0.001
[55]	Singapore	21.0	10	Horizontal, Vertical	1.1	120	27.50,22.00	- -
Our Work	Malaysia	21.8	1	Vertical	1.8	144 193	31.00 -	0.01 0.001

TABLE 4. Comparison of different rain attenuation studies at E-band.

Source	Region	Frequency (GHz)	Period (Year)	Polarization	Distance (km)	Rain Rate (mm/h)	Rain Attenuation (dB)	Time Percentage (%)
[71]	Madrid	73.50	2	Vertical	0.840	20 55	9.00-11.00 15.00-18.00	0.01 0.001
[71]	Madrid	83.50	2	Vertical	0.840	20 55	9.00-11.00 15.00-19.50	0.01 0.001
[72]	South Korea	75.60	3	Vertical	0.100	50 99	28.55 40.48	0.01 0.001
[77]	Sweden	73.50	1	Vertical	1.000	30 35	10.00 12.00	0.02 0.01
[78]	Norway	83.50	1	Vertical	3.450	36 80	22.00 -	0.01 0.001
[76]	Milano	83.00	1	Vertical	0.325	40 120	4.50 9.00	0.01 0.001
[76]	Milano	73.00	1	Vertical	0.325	40 115	4.00 6.50	0.01 0.002
Our Work	Malaysia	73.5	1	Vertical	1.800	108 193	40.10 -	0.03 0.001
Our Work	Malaysia	73.50	1	Vertical	0.300	108 193	20.00 25.00	0.03 0.001

The rain attenuation for this work at 21.8 GHz along 1.8 km vertical polarization link is 31 dB at 0.01% of time. It is mentioning that, the rain attenuation at 0.001% cannot be obtained using our experiment since the link was down when the rain rate was above 180 mm/h. In [69], based on the experimental link in Beijing, China at 23 GHz along 0.7 km vertical polarization, the link went down when the rain rate was above 80 mm/h.

Table 4 presents a comparison of several previous works on rain attenuation at E-band in various regions. To the best of our knowledge, all studies at E-band terrestrial link for long-term rain attenuation statistics (1 year and above) are listed in Table 4. The rain attenuation at 73.5 and 83.5 GHz are comparable based on the rain attenuation along 840 m vertical polarization experimental link in Madrid, Spain [71]. It can be noted that at the high percentage of time 0.01% (low rain rate of 20 mm/h), the maximum rain attenuation values of 11 dB for both bands are the same, as addressed in Table 4. For the high rainfall rate of 55 mm/h at 0.001%, the maximum rain attenuation at 83.5 GHz is 1.5 dB more than the one at 73.5 GHz. In [72], the rain attenuation values at 75.6 GHz over 100 m vertical polarization link are 28.55 and 40.48 dB at the percentages of time 0.01% (rain rate of 50 mm/h) and 0.001% (rain rate of 98.57 mm/h), respectively.

Table 4 shows that the rainfall rate at 0.01% in neighboring Scandinavians countries (Sweden and Norway) are approximately the same [77], [78]. The rain attenuation of 0.01% at 73.5 GHz along 1 km vertical polarization link in Sweden [77] and at 83.5 GHz along 3.45 km vertical polarization link in Norway [78] are comparable. The rain attenuation is 12 dB in 73.5 GHz 1 km link, and 22 dB over 3.5 km link at 83.5 GHz. The 10 dB increase in rain attenuation for the 83.5 GHz could be due to the difference in link distances as the 73.5 GHz has additional 2.5 km.

In [76], the rain attenuation values at 73 and 83 GHz along 325 m are 4 and 4.5 dB, respectively at 0.01% of time with 40 mm/h rainfall rate. This result is the same as [71] which indicates that attenuation at 73 GHz and 83 GHz are comparable. The maximum rain rate obtained from the measurement conducted in Milano, Italy is 120 mm/h at

0.001% of time [76]. In this work, the rain attenuation values are 40.1 and 20 dB at 0.03% of time (108 mm/h rain rate) along the 1.8 km and 300 m vertical polarization links, respectively. The rain attenuation is 25 dB at 0.001% of time (193 mm/h rain rate) in 300 m link, however, the 1.8 km link is down at 0.001% due to the extremely high rain rate. Among the studies in Tables 3 and 4, it can be seen that Malaysia has the highest rainfall rate at 0.01% and 0.001% of time. It is extremely high comparing to the other regions.

X. CONCLUSION

In this work, the rainfall intensity in tropical regions and its effect on the radio propagation at K and E-bands were investigated. An extensive overview for rainfall rate and rain attenuation in different regions around the world was presented. The rain attenuation at 73.5 GHz E-band and 21.8 GHz K-band was calculated based on the measured minimum RSL along 1.8 km experimental links. Moreover, the rain attenuation of the E-band was investigated using two different link paths of 1.8 km and 300 m. The results from this work were compared with several previous works in different regions. From the obtained results, it was found that at 0.01%, the rain rate was 144 mm/h. The maximum rain attenuation for E-band is more than the K-band by 10 dB at 0.03% of time. Moreover, the rain rates of 108 mm/h and above cause an outage for the E-band experimental link of 1.8 km, while for the K-band link with the same distance, the outage occurs when the the rain rate is 180 mm/h and higher. The rain rate of 193 mm/h causes the outage for the shorter E-band link of 300 m. Our findings can be used to support the solution of a multi-band microwave to boost commercial back-haul performances, where the E-band with a large spectrum can be utilized to support high throughput for rain rates below 108 mm/h, while the K-band can take over when the rain rate is higher than 108 mm/h. Finally, it was found that Malaysia, as tropical region, has the highest rainfall rate at 0.01% and 0.001%of time when compared to reported studies in the literature from around the world.

REFERENCES

[1] T. S. Rappaport, Y. Xing, O. Kanhere, S. Ju, A. Madanayake, S. Mandal, A. Alkhateeb, and G. C. Trichopoulos, "Wireless communications and applications above 100 GHz: Opportunities and challenges for 6G and beyond," *IEEE Access*, vol. 7, pp. 78729–78757, 2019.

[2] A. Ghosh, A. Maeder, M. Baker, and D. Chandramouli, "5G evolution: A view on 5G cellular technology beyond 3GPP release 15," *IEEE Access*, vol. 7, pp. 127639–127651, 2019.

[3] G. Hattab, E. Visotsky, M. Cudak, and A. Ghosh, "Toward the coexistence of 5G MmWave networks with incumbent systems beyond 70 GHz," *IEEE Wireless Commun.*, vol. 25, no. 4, pp. 18–24, Aug. 2018.

[4] 3GPP. *Ran Rel-16 Progress and Rel-17 Potential Work Areas*. Accessed: Jul. 2019. [Online]. Available: https://www.3gpp.org/news-events/2058-ran-rel-16-progress-and-rel-17-potential-work-areas

[5] J. Huang, Y. Cao, X. Raimundo, A. Cheema, and S. Salous, "Rain statistics investigation and rain attenuation modeling for millimeter wave short-range fixed links," *IEEE Access*, vol. 7, pp. 156110–156120, 2019.

[6] S. Zang, M. Ding, D. Smith, P. Tyler, T. Rakotoarivelo, and M. A. Kaafar, "The impact of adverse weather conditions on autonomous vehicles: How rain, snow, fog, and hail affect the performance of a self-driving car," *IEEE Veh. Technol. Mag.*, vol. 14, no. 2, pp. 103–111, Jun. 2019.

[7] E. S. Hong, S. Lane, D. Murrell, N. Tarasenko, C. Christodoulou, and J. Keeley, "Estimating rain attenuation at 72 and 84 GHz from raindrop size distribution measurements in Albuquerque, NM, USA," *IEEE Geosci. Remote Sens. Lett.*, vol. 16, no. 8, pp. 1175–1179, Aug. 2019.

[8] X. Boulanger, B. Gabard, L. Casadebaig, and L. Castanet, "Four years of total attenuation statistics of Earth-space propagation experiments at ka-band in Toulouse," *IEEE Trans. Antennas Propag.*, vol. 63, no. 5, pp. 2203–2214, May 2015.

[9] X. Boulanger, B. Benammar, and L. Castanet, "Propagation experiment at Ka-band in French Guiana: First year of measurements," *IEEE Antennas Wireless Propag. Lett.*, vol. 18, no. 2, pp. 241–244, Feb. 2019.

[10] D. Pimienta-Del-Valle, J. M. Riera, and P. Garcia-Del-Pino, "Time and orbital diversity assessment with *ka*-and *q*-band slant-path propagation experiments in Madrid," *IEEE Trans. Antennas Propag.*, vol. 67, no. 2, pp. 1193–1201, Feb. 2019.

[11] Y. H. Lee and S. Winkler, "Effects of rain attenuation on satellite video transmission," in *Proc. IEEE 73rd Veh. Technol. Conf. (VTC Spring)*, May 2011, pp. 1–5.

[12] M. R. Islam, K. Al-Khateeb, F. N. M. Isa, H. Dao, H. M. Salleh, and M. A. M. Ghazali, "Rain induced scintillation measurement on satellite link in tropical climate," in *Proc. Int. Conf. Comput. Commun. Eng.*, Sep. 2014, pp. 181–184.

[13] A. Y. Abdulrahman, T. A. Rahman, M. I. Rafiqul, B. J. Olufeagba, T. A. Abdulrahman, J. Akanni, and S. A. Y. Amuda, "Investigation of the unified rain attenuation prediction method with data from tropical climates," *IEEE Antennas Wireless Propag. Lett.*, vol. 13, pp. 1108–1111, 2014.

[14] L. D. S. Mello and M. S. Pontes, "Unified method for the prediction of rain attenuation in satellite and terrestrial links," *J. Microw., Optoelectron. Electromagn. Appl.*, vol. 11, no. 1, pp. 01–14, Jun. 2012.

[15] *Propagation Data and Prediction Methods Required for the Design of Earth–Space Telecommunications*, document ITU-R P. 618–11, Radiowave propagation, 2013, pp. 1–26.

[16] R. Nalinggam, W. Ismail, and J. S. Mandeep, "Comparison of rain attenuation prediction models with ground measurement data for Penang," *IET Microw., Antennas Propag.*, vol. 5, no. 13, pp. 1546–1551, 2011.

[17] H. Dao, M. R. Islam, and K. Al-Khateeb, "Modification of ITU-R rain fade slope prediction model based on satellite data measured at high elevation angle," *IIUM Eng. J.*, vol. 12, no. 5, pp. 53–59, 2011.

[18] F. Moupfouma, "Rain induced attenuation prediction model for terrestrial and satellite-Earth microwave links," *Annales des Télécommun.*, vol. 42, nos. 9–10, pp. 539–550, 1987.

[19] R. Crane, "Prediction of attenuation by rain," *IEEE Trans. Commun.*, vol. TCOMM-28, no. 9, pp. 1717–1733, Sep. 1980.

[20] M. Cheffena, L. E. Braten, and T. Ekman, "On the space-time variations of rain attenuation," *IEEE Trans. Antennas Propag.*, vol. 57, no. 6, pp. 1771–1782, Jun. 2009.

[21] F. Fedi, "Prediction of attenuation due to rainfall on terrestrial links," *Radio Sci.*, vol. 16, no. 5, pp. 731–743, Sep. 1981.

[22] F. Moupfouma, "Improvement of a rain attenuation prediction method for terrestrial microwave links," *IEEE Trans. Antennas Propag.*, vol. 32, no. 12, pp. 1368–1372, Dec. 1984.

[23] G. E. Mueller, "Propagation of 6-Millimeter waves," *Proc. IRE*, vol. 34, no. 4, pp. 181–183, Apr. 1946.

[24] T. Utsunomiya and M. Sekine, "Rain attenuation at 103 GHz in millimeter wave ranges," *Int. J. Infr. Millim. Waves*, vol. 26, no. 11, pp. 1651–1660, Nov. 2005.

[25] A. Hirata, R. Yamaguchi, H. Takahashi, T. Kosugi, K. Murata, N. Kukutsu, and Y. Kado, "Effect of rain attenuation for a 10-Gb/s 120-GHz-band millimeter-wave wireless link," *IEEE Trans. Microw. Theory Techn.*, vol. 57, no. 12, pp. 3099–3105, Dec. 2009.

[26] A. Hirata, T. Kosugi, H. Takahashi, J. Takeuchi, H. Togo, M. Yaita, N. Kukutsu, K. Aihara, K. Murata, Y. Sato, T. Nagatsuma, and Y. Kado, "120-GHz-band wireless link technologies for outdoor 10-Gbit/s data transmission," *IEEE Trans. Microw. Theory Techn.*, vol. 60, no. 3, pp. 881–895, Mar. 2012.

[27] Y. Yi, H. Jiying, and D. Shuyi, "Rain induced attenuation for 3 mm wave band and its measurement system," *Int. J. Infr. Millim. Waves*, vol. 14, no. 8, pp. 1553–1564, Aug. 1993.

[28] O. Veyrunes, P. Le Clerc, H. Sizun, "First results of precipitation effects at 30, 50, 60 and 94 GHz on a 800 m link in Belfort (France)," in *Proc. IEE Nat. Conf. Antennas Propag.*, 1999, pp. 77–80.

[29] G. E. Weibel and H. O. Dressel, "Propagation studies in millimeter-wave link systems," *Proc. IEEE*, vol. 55, no. 4, pp. 497–513, Apr. 1967.

[30] S. A. Khan, A. N. Tawfik, E. Vilar, and C. J. Gibbins, "Analysis and modelling of rain fade durations at 97 GHz in 6.5 km urban link," *Electron. Lett.*, vol. 36, no. 5, pp. 459–461, 2000.
[31] L. S. Mello, E. Costa, G. Siqueira, N. Dhein, and C. Einloft, "Measurements of rain attenuation in 15 and 18 GHz converging links," in *Proc. 9th Int. Conf. Antennas Propag., (ICAP)*, vol. 2, 1995, pp. 127–130.
[32] A. D. Panagopoulos and J. D. Kanellopoulos, "Statistics of differential rain attenuation on converging terrestrial propagation paths," *IEEE Trans. Antennas Propag.*, vol. 51, no. 9, pp. 2514–2517, Sep. 2003.
[33] L. A. R. da Silva Mello, E. Costa, and R. S. L. de Souza, "Rain attenuation measurements at 15 and 18 GHz," *Electron. Lett.*, vol. 38, no. 4, pp. 197–198, 2002.
[34] *Propagation Data and Prediction Methods Required for the Design of Terrestrial Line-of-Sight Systems*, document ITU-R P. 530–9, Radiowave propagation, 2001, pp. 1–41.
[35] M. S. Pontes, L. da Silva Mello, R. S. L. de Souza, and E. C. B. Miranda, "Review of rain attenuation studies in tropical and equatorial regions in Brazil," in *Proc. 5th Int. Conf. Inf. Commun. Signal Process.*, 2005, pp. 1097–1101.
[36] L. A. R. da Silva Mello, M. S. Pontes, R. M. de Souza, and N. A. P. Garcia, "Prediction of rain attenuation in terrestrial links using full rainfall rate distribution," *Electron. Lett.*, vol. 43, no. 25, pp. 1442–1443, Dec. 2007.
[37] *Propagation Data and Prediction Methods Required for the Design of Terrestrial Line-of-Sight Systems*, document ITU-R P. 530–12, Radiowave propagation, 2006, pp. 1–47.
[38] M. R. Islam, J. Chebil, and A. R. Tharek, "Frequency scaling of rain attenuation from 23-to 38-GHz microwave signals measured in Malaysia," in *Proc. Asia Pacific Microw. Conf. APMC. Microw. Enter 21st Century. Conf.*, vol. 3, Nov./Dec. 1999, pp. 793–796.
[39] M. R. Islam, A. R. Tharek, and J. Chebil, "Comparison between path length reduction factor models based on rain attenuation measurements in Malaysia," in *Proc. Asia–Pacific Microw. Conf.*, Dec. 2000, pp. 1556–1560.
[40] S. C. Sean, J. Din, A. R. Tharek, and M. Z. Abidin, "Studies on characteristics of rain fade at 23 GHz for terrestrial links," in *Proc. Asia–Pacific Conf. Appl. Electromagn. (APACE)*, Aug. 2003, pp. 76–78.
[41] J. S. Mandeep,"Rain attenuation statistics over a terrestrial link at 32.6 GHz at Malaysia," *IET Microw., Antennas Propag.*, vol. 3, no. 7, pp. 1086–1093, Oct. 2009.
[42] A. Y. Abdulrahman, T. A. Rahman, S. K. A. Rahim, and M. R. U. Islam, "Empirically derived path reduction factor for terrestrial microwave links operating at 15 GHz in Peninsula Malaysia," *J. Electromagn. Waves Appl.*, vol. 25, no. 1, pp. 23–37, Jan. 2011.
[43] J. S. Mandeep, O. W. Hui, M. Abdullah, M. Tariqul, M. Ismail, W. Suparta, B. Yatim, P. S. Menon, and H. Abdullah, "Modified ITU-R rain attenuation model for equatorial climate," in *Proc. Proc. IEEE Int. Conf. Space Sci. Commun. (IconSpace)*, Jul. 2011, pp. 89–92.
[44] R. M. Islam, Y. A. Abdulrahman, and T. A. Rahman, "An improved ITU-R rain attenuation prediction model over terrestrial microwave links in tropical region," *EURASIP J. Wireless Commun. Netw.*, vol. 2012, no. 1, p. 189, Dec. 2012.
[45] A. Y. Abdulrahman, T. A. Rahman, S. K. Abdulrahim, and M. R. Islam, "Rain attenuation measurements over terrestrial microwave links operating at 15 GHz in Malaysia," *Int. J. Commun. Syst.*, vol. 25, no. 11, pp. 1479–1488, Nov. 2012.
[46] K. Ulaganathen, T. A. Rahman, S. K. A. Rahim, and R. M. Islam, "Review of rain attenuation studies in tropical and equatorial regions in Malaysia: An overview," *IEEE Antennas Propag. Mag.*, vol. 55, no. 1, pp. 103–113, Feb. 2013.
[47] A. A. Yusuf, A. Falade, B. J. Olufeagba, O. O. Mohammed, and T. A. Rahman, "Statistical evaluation of measured rain attenuation in tropical climate and comparison with prediction models," *J. Microw., Optoelectron. Electromagn. Appl.*, vol. 15, no. 2, pp. 123–134, Jun. 2016.
[48] A. I. O. Yussuff and N. H. H. Khamis, "Modified ITU-R rain attenuation prediction model for a tropical station," *J. Ind. Intell. Inf.*, vol. 1, no. 3, pp. 155–159, 2013.
[49] K. Ulaganathen, M. I. Rafiqul, T. A. Rahman, and M. S. Assis, "Monthly and diurnal variability of rain rate and rain attenuation during the monsoon period in Malaysia," *Radio Eng.*, vol. 23, no. 2, pp. 754–757, 2014.
[50] Y. Abdulrahman, T. A. Rahman, R. M. Islam, B. J. Olufeagba, and J. Chebil, "Comparison of measured rain attenuation in the 10.982-GHz band with predictions and sensitivity analysis," *Int. J. Satell. Commun. Netw.*, vol. 33, no. 3, pp. 185–195, May 2015.
[51] K. Ulaganathen, A. R. Tharek, R. M. Islam, and K. Abdullah, "Case study of rain attenuation at 26 GHz in tropical region (Malaysia) for terrestrial link," in *Proc. IEEE 12th Malaysia Int. Conf. Commun. (MICC)*, Nov. 2015, pp. 252–257.
[52] I. Shayea, T. A. Rahman, M. H. Azmi, and M. R. Islam, "Real measurement study for rain rate and rain attenuation conducted over 26 GHz microwave 5G link system in Malaysia," *IEEE Access*, vol. 6, pp. 19044–19064, 2018.
[53] M. Alhilali, M. Ghanim, J. Din, and H. Y. Lam, "A methodology for precise estimation of rain attenuation on terrestrial millimetre wave links from raindrop size distribution measurements," *Telecommun. Comput. Electron. Control (Telkomnika)*, vol. 17, no. 5, pp. 2139–2164, 2019.
[54] M. Ghanim, M. Alhilali, J. Din, and H. Y. Lam, "Rain attenuation statistics over 5G millimetre wave links in Malaysia," *Indonesian J. Electr. Eng. Comput. Sci.*, vol. 14, no. 2, pp. 1012–1017, 2019.
[55] T.-S. Yee, P.-S. Kooi, M.-S. Leong, and L.-W. Li, "Tropical raindrop size distribution for the prediction of rain attenuation of microwaves in the 10-40 GHz band," *IEEE Trans. Antennas Propag.*, vol. 49, no. 1, pp. 80–83, Jan. 2001.
[56] K. Timothy, S. Sharma, A. Barbara, and M. Devi, "Rain attenuation characteristics—An observational study over LOS microwave link at 11 GHz," *Indian J. Radio Space Phys.*, vol. 23, pp. 130–134, Apr. 1994.
[57] N. Forknall, R. Cole, and D. Webb, "Cumulative fading and rainfall distributions for a 2.1 km, 38 GHz, vertically polarized, line-of-sight link," *IEEE Trans. Antennas Propag.*, vol. 56, no. 4, pp. 1085–1093, Apr. 2008.
[58] R. Olsen, D. Rogers, and D. Hodge, "The aR^b relation in the calculation of rain attenuation," *IEEE Trans. Antennas Propag.*, vol. AP-26, no. 2, pp. 318–329, Mar. 1978.
[59] *Propagation Data and Prediction Methods Required for the Design of Terrestrial Line-of-Sight Systems*, document ITU-R P. 530–11, Radiowave propagation, 2005, pp. 1–45.
[60] A. Aresu, F. Barbaliscia, A. Martellucci, and P. Migliorini, "Rain attenuation statistics on 30 GHz terrestrial link," *Electron. Lett.*, vol. 27, no. 23, pp. 2168–2170, Nov. 1991.
[61] K. S. Paulson and C. J. Gibbins, "Rain models for the prediction of fade durations at millimetre wavelengths," *IEE Proc.-Microw., Antennas Propag.*, vol. 147, no. 6, pp. 431–436, Dec. 2000.
[62] M. O. Fashuyi and T. J. Afullo, "Rain attenuation prediction and modeling for line-of-sight links on terrestrial paths in South Africa," *Radio Sci.*, vol. 42, no. 5, pp. 1–15, Oct. 2007.
[63] M. O. Odedina and T. Afullo, "Characteristics of seasonal attenuation and fading for line-of-sight links in South Africa," in *Proc. SATNAC*, 2008, pp. 203–208.
[64] T. Hirano, J. Hirokawa, and M. Ando, "Estimation of rain rate using measured rain attenuation in the Tokyo tech millimeter-wave model network," in *Proc. IEEE Antennas Propag. Soc. Int. Symp.*, Jul. 2010, pp. 1–4.
[65] P. Thorvaldsen and I. Henne, "Outdoor transmission measurement at 26 GHz: Results of a 4 year trial in Prague," *Radio Sci.*, vol. 51, no. 5, pp. 402–410, May 2016.
[66] S. Shrestha and D.-Y. Choi, "Rain attenuation over terrestrial microwave links in South Korea," *IET Microw., Antennas Propag.*, vol. 11, no. 7, pp. 1031–1039, Jun. 2017.
[67] S. Shrestha and D.-Y. Choi, "Rain attenuation study over an 18 GHz terrestrial microwave link in South Korea," *Int. J. Antennas Propag.*, vol. 2019, pp. 1–16, Mar. 2019.
[68] C. Han, Y. Bi, S. Duan, and G. Lu, "Rain rate retrieval test from 25-GHz, 28-GHz, and 38-GHz millimeter-wave link measurement in Beijing," *IEEE J. Sel. Topics Appl. Earth Observ. Remote Sens.*, vol. 12, no. 8, pp. 2835–2847, Aug. 2019.
[69] C. Han and S. Duan, "Impact of atmospheric parameters on the propagated signal power of millimeter-wave bands based on real measurement data," *IEEE Access*, vol. 7, pp. 113626–113641, 2019.
[70] M. Kyro, V. Kolmonen, and P. Vainikainen, "Experimental propagation channel characterization of mm-wave radio links in urban scenarios," *IEEE Antennas Wireless Propag. Lett.*, vol. 11, pp. 865–868, 2012.
[71] J. M. Garcia-Rubia, E. Riera, P. Garcia-del-Pino, and A. Benarroch, "Attenuation measurements and propagation modeling in the W-Band," *IEEE Trans. Antennas Propag.*, vol. 61, no. 4, pp. 1860–1867, Apr. 2013.
[72] S. Shrestha and D.-Y. Choi, "Rain attenuation statistics over millimeter wave bands in South Korea," *J. Atmos. Solar-Terrestrial Phys.*, vols. 152–153, pp. 1–10, Jan. 2017.

[73] F. Norouzian, E. Marchetti, M. Gashinova, E. Hoare, C. Constantinou, P. Gardner, and M. Cherniakov, "Rain attenuation at millimeter wave and low-THz frequencies," *IEEE Trans. Antennas Propag.*, vol. 68, no. 1, pp. 421–431, Jan. 2020.

[74] U. J. Lewark, T. Mahler, J. Antes, F. Boes, A. Tessmann, R. Henneberger, I. Kallfass, and T. Zwick, "Experimental validation of heavy rain attenuation in E-band based on climate wind tunnel measurements at 77 GHz," *CEAS Space J.*, vol. 7, no. 4, pp. 475–481, Dec. 2015, doi: 10.1007/s12567-015-0100-6.

[75] L. Luini, G. Roveda, M. Zaffaroni, M. Costa, and C. Riva, "EM wave propagation experiment at E band and D band for 5G wireless systems: Preliminary results," in *Proc. 12th Eur. Conf. Antennas Propag. (EuCAP)*, Apr. 2018, pp. 1–5.

[76] L. Luini, G. Roveda, M. Zaffaroni, M. Costa, and C. Riva, "The impact of rain on short E-band radio links for 5G mobile systems: Experimental results and prediction models," *IEEE Trans. Antennas Propag.*, to be published.

[77] J. Hansryd, Y. Li, J. Chen, and P. Ligander, "Long term path attenuation measurement of the 71–76 GHz band in a 70/80 GHz microwave link," in *Proc. 4th Eur. Conf. Antennas Propag.*, Apr. 2010, pp. 1–4.

[78] T. Tjelta and T. O. Breivik, "Measured attenuation data and predictions for a Gigabit radio link in the 80 GHz band," in *Proc. 3rd Eur. Conf. Antennas Propag.*, Mar. 2009, pp. 657–661.

[79] *Characteristics of Precipitation for Propagation Modelling*, document ITU-R PN. 837–1, Radiowave propagation, 1994, pp. 1–4.

[80] *Characteristics of Precipitation for Propagation Modelling*, document ITU-R P. 837–7, Radiowave propagation, 2017, pp. 1–8.

[81] *Propagation Data and Prediction Methods Required for the Design of Terrestrial Line-of-Sight Systems*, document ITU-R P. 530–17, Radiowave propagation, 2017, pp. 1–59.

[82] M. F. Charles and J. R. David. (1973). *Rainfall Intensity Instruments and Measurements*. [Online]. Available: https://scholarspace.manoa.hawaii.edu/bitstream/10125/18102/1/wrrctr67.pdf

[83] L. W. Larson and E. L. Peck, "Accuracy of precipitation measurements for hydrologic modeling," *Water Resour. Res.*, vol. 10, no. 4, pp. 857–863, Aug. 1974.

[84] R. J. Doviak, *Doppler Radar and Weather Observations*. North Chelmsford, MA, USA: Courier Corporation, 2006.

[85] A. Fauziana, U. Tomoki, and S. Takahiro. (2017). *Determination of Z-R Relationship and Inundation Analysis for Kuantan Rive Basin*. [Online]. Available: http://www.met.gov.my/penerbitan/kertasteknikal

[86] G. Skofronick-Jackson, W. A. Petersen, W. Berg, C. Kidd, E. F. Stocker, D. B. Kirschbaum, R. Kakar, S. A. Braun, G. J. Huffman, T. Iguchi, P. E. Kirstetter, C. Kummerow, R. Meneghini, R. Oki, W. Olson, Y. N. Takayabu, K. Furukawa, and T. Wilheit, "The global precipitation measurement (GPM) mission for science and society," *Bull. Amer. Meteorolog. Soc.*, vol. 98, no. 8, pp. 1679–1695, 2017.

[87] Q. Sun, C. Miao, Q. Duan, H. Ashouri, S. Sorooshian, and K. Hsu, "A review of global precipitation data sets: Data sources, estimation, and intercomparisons," *Rev. Geophys.*, vol. 56, no. 1, pp. 79–107, Mar. 2018.

[88] P. A. Owolawi and T. J. Afullo, "Rainfall rate modeling and worst month statistics for millimetric line-of-sight radio links in South Africa," *Radio Sci.*, vol. 42, no. 6, pp. 1–11, Dec. 2007.

[89] T. V. Omotosho, O. O. Ometan, S. A. Akinwumi, O. M. Adewusi, A. O. Boyo, and M. S. J. Singh, "Year to year variation of rainfall rate and rainfall regime in Ota, Southwest Nigeria for the year 2012 to 2015," *J. Phys., Conf. Ser.*, vol. 852, no. 1, May 2017, Art. no. 012013.

[90] I. Md Rafiqul, M. M. Alam, A. K. Lwas, and S. Y. Mohamad, "Rain rate distributions for microwave link design based on long term measurement in Malaysia," *Indonesian J. Electr. Eng. Comput. Sci.*, vol. 10, no. 3, pp. 1023–1029, 2018.

[91] P. Rice and N. Holmberg, "Cumulative time statistics of surface-point rainfall rates," *IEEE Trans. Commun.*, vol. 21, no. 10, pp. 1131–1136, Oct. 1973.

[92] F. A. Huff, "Time distribution characteristics of rainfall rates," *Water Resour. Res.*, vol. 6, no. 2, pp. 447–454, Apr. 1970.

[93] S. H. Lin, "Rain-rate distributions and extreme-value statistics," *Bell Syst. Tech. J.*, vol. 55, no. 8, pp. 1111–1124, Oct. 1976.

[94] S. H. Lin, "More on rain rate distributions and extreme value statistics," *Bell Syst. Tech. J.*, vol. 57, no. 5, pp. 1545–1568, May 1978.

[95] B. Segal, "An analytical examination of mathematical models for the rainfall rate distribution function," *Annales des Télécommun.*, vol. 35, nos. 11–12, pp. 434–438, 1980.

[96] F. Moupfouma, L. Martin, N. Spanjaard, and K. Hughes, "Rainfall rate characteristics for microwave systems in tropical and equatorial areas," *Int. J. Satell. Commun.*, vol. 8, no. 3, pp. 151–161, May 1990.

[97] D. Salisu, S. Supiah, and A. Azmi, "Modeling the distribution of rainfall intensity using hourly data," *Amer. J. Environ. Sci.*, vol. 6, no. 3, pp. 238–243, Mar. 2010.

[98] A. Maitra, A. De, and A. Adhikari, "Rain and rain-induced degradations of satellite links over a tropical location," *IEEE Trans. Antennas Propag.*, vol. 67, no. 8, pp. 5507–5518, Aug. 2019.

[99] O. O. Ometan, T. V. Omotosho, S. A. Akinwumi, M. O. Adewusi, and A. O. Boyo, "Dataset of daily variation of rain rate distribution at Ota in Southwest Nigeria," *Data Brief*, vol. 25, Aug. 2019, Art. no. 104154.

[100] T. P. Roderick, C. Wasko, and A. Sharma, "Atmospheric moisture measurements explain increases in tropical rainfall extremes," *Geophys. Res. Lett.*, vol. 46, no. 3, pp. 1375–1382, Feb. 2019.

[101] M. C. Kestwal, S. Joshi, and L. S. Garia, "Prediction of rain attenuation and impact of rain in wave propagation at microwave frequency for tropical region (Uttarakhand, India)," *Int. J. Microw. Sci. Technol.*, vol. 2014, pp. 1–6, Jun. 2014.

[102] F. Giannetti, R. Reggiannini, M. Moretti, E. Adirosi, L. Baldini, L. Facheris, A. Antonini, S. Melani, G. Bacci, A. Petrolino, and A. Vaccaro, "Real-time rain rate evaluation via satellite downlink signal attenuation measurement," *Sensors*, vol. 17, no. 8, p. 1864, 2017.

[103] I. Shayea, T. A. Rahman, M. H. Azmi, and A. Arsad, "Rain attenuation of millimetre wave above 10 GHz for terrestrial links in tropical regions," *Trans. Emerg. Telecommun. Technol.*, vol. 29, no. 8, Aug. 2018, Art. no. e3450.

[104] J. Roche, H. Lake, D. Worthington, C. Tsao, and J. DeBettencourt, "Radio propagation at 27-40 GHz," *IEEE Trans. Antennas Propag.*, vol. 18, no. 4, pp. 452–462, Jul. 1970.

[105] K. M. M. Navarro, E. Costa, C. A. M. Rodriguez, S. Cruz-Pol, and L. V. L. Colon, "Realistic rain model for the estimation of the rainfall rate from radar measurements," *IEEE Trans. Antennas Propag.*, vol. 67, no. 9, pp. 6104–6114, Sep. 2019.

[106] D. Nandi and A. Maitra, "The effects of rain on millimeter wave communication for tropical region," in *Proc. URSI Asia–Pacific Radio Sci. Conf. (AP-RASC)*, Mar. 2019, pp. 1–3.

[107] C. Bostian, W. Stutzman, P. H. Wiley, and R. Marshall. (1974). *The Influence of Polarization on Millimeter Wave Propagation Through Rain*. [Online]. Available: https://scholarspace.manoa.hawaii.edu/bitstream/10125/18102/1/wrrctr67.pdf

[108] T. S. Chu, "Rain-induced cross-polarization at centimeter and millimeter wavelengths," *Bell Syst. Tech. J.*, vol. 53, no. 8, pp. 1557–1579, Oct. 1974.

[109] M. Thurai, K. V. Mishra, V. N. Bringi, and W. F. Krajewski, "Initial results of a new composite-weighted algorithm for dual-polarized X-band rainfall estimation," *J. Hydrometeorol.*, vol. 18, no. 4, pp. 1081–1100, Apr. 2017.

[110] T. N. Rao, K. Amarjyothi, and S. V. B. Rao, "Attenuation relations for monsoonal rain at the X band from disdrometric measurements: Dependency on temperature, raindrop size distribution and drop shape models," *Quart. J. Roy. Meteorolog. Soc.*, vol. 144, no. 1, pp. 64–76, Nov. 2018.

[111] D. Wolfensberger, M. Gabella, A. Berne, and U. Germann, "Potential use of specific differential propagation phase delay for the retrieval of rain rates in strong convection over switzerland," in *Proc. 11th Int. Workshop Precipitation Urban Areas (UrbanRain18)*, 2019, pp. 1–7.

[112] A. Overeem, H. Leijnse, and R. Uijlenhoet, "Two and a half years of country-wide rainfall maps using radio links from commercial cellular telecommunication networks," *Water Resour. Res.*, vol. 52, no. 10, pp. 8039–8065, Oct. 2016.

[113] A. Overeem, H. Leijnse, and R. Uijlenhoet, "Country-wide rainfall maps from cellular communication networks," *Proc. Nat. Acad. Sci. USA*, vol. 110, no. 8, pp. 2741–2745, Feb. 2013.

[114] O. Goldshtein, H. Messer, and A. Zinevich, "Rain rate estimation using measurements from commercial telecommunications links," *IEEE Trans. Signal Process.*, vol. 57, no. 4, pp. 1616–1625, Apr. 2009.

[115] F. Fenicia, L. Pfister, D. Kavetski, P. Matgen, J.-F. Iffly, L. Hoffmann, and R. Uijlenhoet, "Microwave links for rainfall estimation in an urban environment: Insights from an experimental setup in Luxembourg-city," *J. Hydrol.*, vols. 464–465, pp. 69–78, Sep. 2012.

[116] A. Overeem, H. Leijnse, and R. Uijlenhoet, "Measuring urban rainfall using microwave links from commercial cellular communication networks," *Water Resour. Res.*, vol. 47, no. 12, Dec. 2011.

[117] H. Messer and O. Sendik, "A new approach to precipitation monitoring: A critical survey of existing technologies and challenges," *IEEE Signal Process. Mag.*, vol. 32, no. 3, pp. 110–122, May 2015.
[118] J. Ostrometzky, D. Cherkassky, and H. Messer, "Accumulated mixed precipitation estimation using measurements from multiple microwave links," *Adv. Meteorol.*, vol. 2015, pp. 1–9, Apr. 2015.
[119] J. Ostrometzky and H. Messer, "Accumulated rainfall estimation using maximum attenuation of microwave radio signal," in *Proc. IEEE 8th Sensor Array Multichannel Signal Process. Workshop (SAM)*, Jun. 2014, pp. 193–196.
[120] J. de Bettencourt, "Statistics of terrestrial millimeter-wave rainfall attenuation," Raytheon Co., Waltham, MA, USA, Tech. Rep., 1973.
[121] R. K. Crane, "Prediction of the effects of rain on satellite communication systems," *Proc. IEEE*, vol. 65, no. 3, pp. 456–474, Mar. 1977.
[122] *Specific Attenuation Model for Rain for Use in Prediction Methods*, document ITU-R P. 838–3, Radiowave propagation, 2005, pp. 1–8.
[123] E. Regonesi, L. Luini, and C. Riva, "Limitations of the ITU-R P.838-3 model for rain specific attenuation," in *Proc. 13th Eur. Conf. Antennas Propag. (EuCAP)*, Mar./Apr. 2019, pp. 1–4.
[124] E. S. Hong, S. Lane, D. Murrell, N. Tarasenko, and C. Christodoulou, "Mitigation of reflector dish wet antenna effect at 72 and 84 GHz," *IEEE Antennas Wireless Propag. Lett.*, vol. 16, pp. 3100–3103, 2017.
[125] B. Blevis, "Losses due to rain on radomes and antenna reflecting surfaces," *IEEE Trans. Antennas Propag.*, vol. 13, no. 1, pp. 175–176, Jan. 1965.
[126] M. R. Islam and A. R. Tharek, "Measurement of wet antenna effect on microwave propagation at 23, 26 and 38 GHz," in *Proc. IEEE Antennas Propag. Soc. Int. Symp. Transmitting Waves Progr. Next Millennium. Dig. Held Conjunct, USNC/URSI Nat. Radio Sci. Meeting*, vol. 4, Jul. 2000, pp. 2094–2098.
[127] M. M. Z. Kharadly and R. Ross, "Effect of wet antenna attenuation on propagation data statistics," *IEEE Trans. Antennas Propag.*, vol. 49, no. 8, pp. 1183–1191, Aug. 2001.
[128] H. Leijnse, R. Uijlenhoet, and J. N. M. Stricker, "Microwave link rainfall estimation: Effects of link length and frequency, temporal sampling, power resolution, and wet antenna attenuation," *Adv. Water Resour.*, vol. 31, no. 11, pp. 1481–1493, Nov. 2008.
[129] S. K. A. Rahim, A. Y. Abdulrahman, T. A. Rahman, and M. R. U. Islam, "Measurement of wet antenna losses on 26 GHz terrestrial microwave link in Malaysia," *Wireless Pers. Commun.*, vol. 64, no. 2, pp. 225–231, May 2012.
[130] M. Schleiss, J. Rieckermann, and A. Berne, "Quantification and modeling of wet-antenna attenuation for commercial microwave links," *IEEE Geosci. Remote Sens. Lett.*, vol. 10, no. 5, pp. 1195–1199, Sep. 2013.
[131] N. David, O. Harel, P. Alpert, and H. Messer, "Study of attenuation due to wet antenna in microwave radio communication," in *Proc. IEEE Int. Conf. Acoust., Speech Signal Process. (ICASSP)*, Mar. 2016, pp. 4418–4422.
[132] J. Ostrometzky, R. Raich, L. Bao, J. Hansryd, and H. Messer, "The wet-antenna effect—A factor to be considered in future communication networks," *IEEE Trans. Antennas Propag.*, vol. 66, no. 1, pp. 315–322, Jan. 2018.
[133] M. Fencl, P. Valtr, M. Kvicera, and V. Bares, "Quantifying wet antenna attenuation in 38-GHz commercial microwave links of cellular backhaul," *IEEE Geosci. Remote Sens. Lett.*, vol. 16, no. 4, pp. 514–518, Apr. 2019.
[134] P. Valtr, M. Fencl, and V. Bares, "Excess attenuation caused by antenna wetting of terrestrial microwave links at 32 GHz," *IEEE Antennas Wireless Propag. Lett.*, vol. 18, no. 8, pp. 1636–1640, Aug. 2019.
[135] M. Mishra, *Encyclopedia of Polymer Applications, 3 Volume Set*. Boca Raton, FL, USA: CRC Press, 2018.
[136] S. H. Lin, "11-GHz radio: Nationwide long-term rain rate statistics and empirical calculation of 11-GHz microwave rain attenuation," *Bell Syst. Tech. J.*, vol. 56, no. 9, pp. 1581–1604, Nov. 1977.
[137] F. Moupfouma, "Electromagnetic waves attenuation due to rain: A prediction model for terrestrial or LOS SHF and EHF radio communication links," *J. Infr., Millim., Terahertz Waves*, vol. 30, no. 6, pp. 622–632, Jun. 2009.
[138] ERICSSON. (2017). *Mini-Link 6363 Data Sheet*. [Online]. Available: https://tele-a.ru/wp-content/uploads/2017/07/6363-datasheet.pdf
[139] ERICSSON. (2015). *Mini-Link 6352 Data Sheet*. [Online]. Available: http://telea.ru/wp-content/uploads/2015/09/6352-DS.pdf
[140] H. R. Gauge. (2016). *Rainfall Data Logging System*. [Online]. Available: https://www.onsetcomp.com/files/datasheet/Onset%20HOBO%20RG3%20Rain%20Gauge.pdf
[141] D. Pimienta-del-Valle, J. M. Riera, P. Garcia-del-Pino, and G. A. Siles, "Three-year fade and inter-fade duration statistics from the Q-band Alphasat propagation experiment in Madrid," *Int. J. Satell. Commun. Netw.*, vol. 37, no. 5, pp. 460–476, Sep. 2019.
[142] D. Cherkassky, J. Ostrometzky, and H. Messer, "Precipitation classification using measurements from commercial microwave links," *IEEE Trans. Geosci. Remote Sens.*, vol. 52, no. 5, pp. 2350–2356, May 2014.
[143] L. Bao, C. Larsson, M. Mustafa, J. Selin, J. C. M. Andersson, J. Hansryd, M. Riedel, and H. Andersson, "A brief description on measurement data from an operational microwave network in Gothenburg, Sweden," in *Proc. 15th Int. Conf. Environ. Sci. Technol.*, Rhodes, Greece, vol. 31, 2017, pp. 1–5.
[144] J. Ostrometzky and H. Messer, "Dynamic determination of the baseline level in microwave links for rain monitoring from minimum attenuation values," *IEEE J. Sel. Topics Appl. Earth Observ. Remote Sens.*, vol. 11, no. 1, pp. 24–33, Jan. 2018.
[145] F.-W. Chen and C.-W. Liu, "Estimation of the spatial rainfall distribution using inverse distance weighting (IDW) in the middle of Taiwan," *Paddy Water Environ.*, vol. 10, no. 3, pp. 209–222, Sep. 2012, doi: 10.1007/s10333-012-0319-1.
[146] P. Longley, M. Goodchild, D. Maguire, and D. Rhind, *Geographic Information Systems and Science*. Hoboken, NJ, USA: Wiley, 2001, pp. 150–151.
[147] P. A. Burrough, R. McDonnell, R. A. McDonnell, and C. D. Lloyd, *Principles of Geographical Information Systems*. Oxford, U.K.: Oxford Univ. Press, 2015.
[148] H. Zhu and S. Jia, "Uncertainty in the spatial interpolation of rainfall data," *Progr. Geography*, vol. 23, no. 2, pp. 34–42, 2004.
[149] X. Lin and Q. Yu, "Study on the spatial interpolation of agroclimatic resources in Chongqing," *J. Anhui Agricult. Sci.*, vol. 36, no. 30, pp. 13431–13463, 2008.
[150] J. Chebil and T. A. Rahman, "Rain rate statistical conversion for the prediction of rain attenuation in Malaysia," *Electron. Lett.*, vol. 35, no. 12, pp. 1019–1021, 1999.

AHMED M. AL-SAMAN received the B.S. degree in electrical-electronics and telecommunications engineering from IBB University, Yemen, in 2004, and the M.Eng. and Ph.D. degrees in electrical-electronics and telecommunications engineering from Universiti Teknologi Malaysia (UTM), Malaysia, in 2013 and 2017, respectively. From July 2017 to July 2019, he held a postdoctoral position with the Innovation Centre for 5G (IC5G), UTM, Malaysia. He is currently conducting a postdoctoral research with the Department of Manufacturing and Civil Engineering, Norwegian University of Science and Technology (NTNU). From 2004 to 2010, he was an Engineer with the Department of Management of Frequency Spectrum, Ministry of Communications and Information Technology, Yemen. His research interests are in the area of signal processing, channel propagation, UWB systems, and millimeter wave communication for 5G systems.

MICHAEL CHEFFENA received the M.Sc. degree in electronics and computer technology from the University of Oslo, Oslo, Norway, in 2005, and the Ph.D. degree in telecommunications from the Norwegian University of Science and Technology (NTNU), Trondheim, Norway, in 2008. He was a Visiting Researcher with the Communications Research Center, Ottawa, ON, Canada, in 2007. From 2009 to 2010, he conducted his postdoctoral study at the University Graduate Center, Kjeller, Norway, and the French Space Agency, Toulouse, France. He is currently a Full Professor with NTNU. His current research interests include the modeling and prediction of radio channels for both terrestrial and satellite links.

MARSHED MOHAMED received the M.Sc. degree in electrical engineering with emphasis on radio communication from the Blekinge Institute of Technology, Sweden, and the Ph.D. degree in electronics and telecommunication from the Norwegian University of Science and Technology (NTNU), Norway. He was also a Visiting Researcher with the Department of Information Technology, Ghent University, Belgium. He is currently working in wireless sensor networks with NTNU as a Postdoctoral Fellow. His current research interest also includes the broad areas of wireless communications with focuses on radio propagation.

MARWAN HADRI AZMI received the B.Eng. degree (Hons.) in electrical and telecommunications from Universiti Teknologi Malaysia, Johor Bahru, Malaysia, in 2003, the M.Sc. degree in communications and signal processing from the Imperial College of Science, Technology and Medicine, University of London, in 2005, and the Ph.D. degree from the University of New South Wales, Australia, in 2012. From 2012 to 2014, he spent his sabbatical leave of absence with McGill University, Canada, working in the funded project by RIM, Inc., and NSERC, Cooperative Spectrum Sensing, and Information Relaying in Cognitive Wireless Communications. He is currently a Senior Lecturer with the Wireless Communication Centre, Universiti Teknologi Malaysia. His research interests include mobile and wireless communications, communication theory, error control coding, relay networks, spectrum sensing for cognitive radio, and iterative receiver.

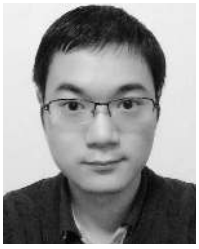

YUN AI received the M.Sc. degree in electrical engineering from the Chalmers University of Technology, Göteborg, Sweden, in 2012, and the Ph.D. degree from the University of Oslo, Oslo, Norway, in 2018. In 2016, he was a Visiting Researcher with the Department of Information and Computer Science, Keio University, Tokyo, Japan. In 2016, funded by a stipend from the Norwegian University Center, Saint Petersburg, Russia, he was a Visiting Researcher with the Faculty of Applied Mathematics and Control Processes, Saint Petersburg State University, Saint Petersburg, Russia. He is currently a Researcher with the Norwegian University of Science and Technology (NTNU), Norway. He has also been with the Signal Processing Group, Technische Universität Darmstadt, Darmstadt, Germany, as a Research Student and also with Ericsson as an Engineer. His current research interests include the broad areas of wireless communications with focuses on communication theory, wireless sensor networks, and smart grid.